Everything I think you should know about Inverse Adding-Doubling

Scott Prahl*

April 2024

Abstract

This document describes a method for measuring the optical properties of scattering and absorbing materials. The general idea is that you have made careful measurements of the total reflection and transmission of the sample. These observations are then fed into a program (the inverse adding-doubling `iad` program) to extract the intrinsic optical parameters for the sample. The program does this by repeatedly guessing the optical properties and comparing the expected observables with those that you have made. Upon matching, voilà, those optical properties used to generate the expected observables are the ones that characterize your sample.

If only it were that simple. I have written a couple of papers on the details of the program [1–3], on optical properties in general [4], and on making those measurements with integrating spheres [5, 6]. Unfortunately, not one of these brings all the pieces together. Partly, this is my fault, partly it is because none of the articles is really concerned with dotting all the i's and crossing all the t's, partly it is because an appropriate forum for this information just doesn't exist other than in this manual.

This document describes version 3.16.2 of the `iad`. The program is documented in the journal article [7].

Every once in a while, users of `iad` let me know about some odd behavior in the program. Sometimes it is a bug in the program and sometimes it is their data. For the first few months of 2024, I have been reviewing the entire program and making multiple improvements that improve the robustness and utility of `iad`.

The last time I looked closely at the program was in 2011 when Ville Keränen somehow managed to break the damn program essentially every week for a full year. As a consequence, `iad` is much more robust than it has ever been before.

---

*Oregon Tech, EERE, 27500 SW Parkway Ave., Wilsonville, OR 97225, (503) 821-1344 (office), email: scott.prahl@oit.edu https://omlc.org

Contents

Sphere Properties

A	area	mm^2
a	area divided by the total sphere wall area	—
X_d	(subscript d) detector	—
X_w	(subscript w) sphere wall	—
X_e	(subscript t) third port	—
X_s	(subscript s) sample	—
X_b	(subscript b) beam	—

Sample Properties

δ	sample thickness	mm
μ_a	absorption coefficient	mm^{-1}
μ_s	scattering coefficient	mm^{-1}
g	anisotropy, (average cosine of phase function)	—
μ_s'	reduced scattering coefficient $= \mu_s(1-g)$	mm^{-1}

Idealized Values

r	true reflectance	—
t	true transmittance	—

Observables

R	unnormalized reflection	arbitrary
T	unnormalized transmission	arbitrary
U	unnormalized unscattered transmission	arbitrary
M_R	measured total reflectance (eq. 2)	—
M_T	measured total transmittance (eq. 3)	—
M_U	measured unscattered transmittance (eq. 6)	—
X_0	(subscript 0) empty or nothing	—
X_{100}	(subscript 100) all	—
X_{std}	(subscript std) reflectance standard	—
X_{dark}	(subscript $dark$) blocked beam	—
$X^{diffuse}$	(superscript $diffuse$) diffuse illumination (generally omitted)	—
X^{direct}	(superscript $direct$) direct or normal illumination	—

Table 1: Nomenclature used in this document. For example, A_s is the area of the sample port and a_d is $A_d/(A_w + A_e + A_s + A_d)$. The symbol r_s^{direct} describes the true reflectance from the sample for direct (normal) illumination and r_s is the sample reflectance for diffuse illumination (where the *diffuse* superscript has been omitted).

1 Introduction

Inverse adding-doubling is a method for generating the optical properties of scattering and absorbing materials. Reflection and transmission measurements (typically made with an integrating sphere) are converted to the optical properties of the sample (scattering, absorption, and anisotropy) using the computer program `iad`. The `iad` has been extensively tested and validated for accuracy and precision; it is widely used [6, 8–110].

1.1 Overview

To use the `iad` program, create a data file with the appropriate header for your experiment and then append your your experimental measurements of reflectance and transmittance. If the file is called `data.rxt`[1] then the file can be processed by the `iad` program by typing

```
prompt> iad data
```

You'll get back a file `data.txt` that contains a set of optical properties—the scattering, absorption, and anisotropy coefficients that correspond to each measurement set.

The `iad` program finds the optical properties characterizing a sample by using the measured total reflectance M_R, the measured total transmittance M_T values, and potentially the measured unscattered transmittance values M_U. A set of optical properties is guessed and values for M_R and M_T are calculated. These values are compared with the measured values. If they match then the optical properties for the sample have been found. If they do not match then a new set of optical properties is guessed and the process is repeated. As van de Hulst pointed out, the approach is fairly brute force. Oh, well it works.

The `iad` program has a number of parameters that can be modified to account for different experimental situations. One, two, or three measurements can be used to determine one, two, or three optical properties. `iad` is intended to be used from the command line. The processed output file contains a summary of the experimental conditions as well as all the calculated optical properties.[2]

1.2 Assumptions

The adding-doubling method is used to calculate reflectance and transmittance. Since the adding-doubling method is an accurate solution of the radiative transport equation for all albedos, all optical depths, and all phase functions this method can be applied to any medium for which the radiative transport equation is valid. However, a number of restrictions apply

---

[1]The `.rxt` extension is the default extension for data files to be processed by this program. Any other extension is permitted, but you will have to type it out completely (e.g., `iad data.dat`).

[2]The optical properties are readily graphed using `gnuplot` or `python` because all the comment lines at the top of the file are preceded by a hash mark (`#`).

1. distribution of light is independent of time,

2. samples have homogeneous optical properties,

3. tissue geometry is an infinite plane-parallel slab,

4. boundaries are smooth,

5. internal reflectance is governed by Fresnel's law, and

6. polarization effects may be ignored.

Despite these constraints, inverse adding-doubling has a number of positive features

1. works for any combination of optical properties.

2. takes into account all the interactions of a sample sandwiched between glass slides

3. incorporates the effects of the integrating spheres on the measured values

4. accounts for lost light (light that is not collected by the spheres)

5. has a reasonable trade-off between accuracy and speed.

1.3 Background

The graduate student days

The `iad` program started its life as an inverse diffusion equation program.Steve Jacques (then at the Wellman Laboratories of Photomedicine) and I (a graduate student at the University of Texas at Austin) wanted a way to find the optical properties of tissues based on observed quantities. We published a paper [1] and thought that was that. We subsequently discovered that the diffusion model can generate negative reflectances (!!) for samples with strongly anisotropic scattering ($g = 0.9$). Steve encouraged me to improve the inverse diffusion program. I subsequently improved that program in two important ways. First, I adapted the diffusion code to the δ-Eddington approximation to eliminate the problem with highly anisotropic scattering. Second, I replaced my simple-minded minimization method with the simplex method of Nelder and Weaver. I used the inverse δ-Eddington model in my 1982 thesis supervised by the Dr. Jon Valvano and the late Dr. A. J. Welch.

The post-doc era

About the time I was giving my final defense I realized that I could not recommend my inverse program to anyone because I had no idea how accurate it was. The δ-Eddington model is a good solution to the radiative transport equation but it only uses the first two terms of the infinite series of spherical Legendre

polynomials. I started working on a paper to estimate the errors but it seemed pretty pointless.

Instead of continuing, I decided to use the adding-doubling program (which can use an arbitrary number of spherical Legendre polynomials) that I had included in a different section of my thesis to replace the δ-Eddington program in the inverse algorithm. This led to the inverse adding-doubling (`iad`) program. This was done in 1983 in Amsterdam under the auspices of Dr. Martin van Gemert and the necessary guilders came from the Fundamenteel Onderzoek voor Materie. This program was much more accurate. In fact, you can make the adding-doubling method as accurate as desired by increasing the number of quadrature points. The major improvement to the adding-doubling implementation was to incorporate mismatched boundaries. Initially my solution was curiously inaccurate. Eventually, I realized that an accurate implementation required breaking the angular integration into two parts: one part over all totally internally reflected angles and the other part over the angles that escape the sample.

One implementation challenge is the selection of initial optical properties for use as guesses. Starting with poor guesses can easily lead to convergence at a local minimum, thereby missing the desired global minimum. In 1984, I spent a week working with Steve Jacques at the M.D. Anderson Cancer Center in Houston, attempting to address this issue.

Choosing initial values is akin to approximately solving the entire inverse problem. I eventually adopted the δ-Eddington method to generate starting values. Further refinement of the starting routine occurred over a couple of months at the University of Utah Laser Institute in Salt Lake City, with generous support from Dr. Richard Straight. Here, the starting routine was completely rewritten. There I developed heuristics for calculating starting values, which were later published in the adding-doubling paper [2]. Large portions of the code were modularized into smaller files, and the first version of this documentation was drafted. After considerable refinement—quite a lot, in fact—this method remained in use until 2004.

While I worked at Wellman Laboratories (1984-1985) in Boston as a post-doc under Dr. Rox Anderson, I fixed a number of minor bugs and adapted the header for the input data files to bring the sphere corrections into accordance with the integrating sphere paper I worked on with Pickering and others.

Version 1.0.0 — The beginning

Until this stage, `iad` was developed in Pascal. I must confess, despite its waning popularity, I had a fondness for Pascal. By 1986, however, it was becoming increasingly difficult to find robust Pascal compilers, as Pascal had fallen out of favor. The programming community had shifted its preference to C.

Simultaneously, I became fascinated with the exceptional typesetting capabilities of TeX—the same system used to compose this document. Given that `iad` is mathematically complex, I desired aesthetically pleasing and clear

typesetting for my comments. This led me to adopt the [3], which allows for the creation of elegant documentation, albeit at the expense of a preprocessing step.

Upon joining the Oregon Medical Laser Center, one of my initial tasks was to convert the entire program to ANSI C. This conversion not only modernized `iad` but also enhanced its speed and reliability, for instance, through the implementation of a stored-grid approach. This effort was supported by the Collins Foundation and concluded in the early 1990s.

The stored-grid addresses the initial guess problem. This is, once again, a brute-force approach that is done before the inversion process starts. So, for example, when the albedo a and optical thickness b are being sought, I create a grid of a and b values and store the reflection and transmission values for each grid point. The initial guesses for the inversion process are the values of a and b that most closely match the measured reflection and transmission. This finally solved the local versus global minimum problem once and for all.

The stored-grid results in much faster solutions when the sample has constant values from point to point. So, as long as the anisotropy remains constant, the a and b grid gives starting values that rapidly converge to the desired values. On the other hand, when the unscattered transmission is also measured, then the optical thickness b will change for every point — meaning that the a and g grid must be recalculated for each new value of b. Despite being slower, having starting values that converge to the correct global minimum is a crucial improvement.

User Issues 1

The next stage in the life of this program has been due to my most excellent interaction with Dr. David Royston then at the FDA [111]. He did many careful experiments and kept asking what was going wrong. This led to a rapid series of `iad` releases as I addressed shortcomings in the program.

David provided the incentive to incorporate light absorption by slides sandwiching the sample. This feature becomes important in the near-IR and solved a user problem twenty years later![4]

Version 2.0.0 — Repackaging

In the intervening ten years or so, I would correspond with users and add features or fix bugs as needed. In 2004, I looked at the code base and realized that I had added stuff (multiple-layers, conical irradiation) and that compiling the code was a huge hassle. This led to version 2.0.0 — the first major version increase. For this release, I reorganized the code base and cleaned up the build process. Then I discovered that this document was severely out of date. I ignored the urge to update it.

---

[3] CWEB system

[4] This functionality is accessed through the `-E` command-line option.

Trouble!

In 2006, I needed to revisit the whole problem of measuring optical properties. I had a contract to build a bunch of optical phantoms with closely specified tolerances for optical properties. We made a bunch of measurements to show that the optical properties were the same as the promised ones. These measurements included two thicknesses of identical polyurethane material as well as on phantoms with the same scattering coefficient, but with different absorbing properties. Unfortunately not all of these measurements were consistent!

I knew that the optical properties derived by `iad` required careful measurements using integrating spheres. We made obsessively careful measurements but the results were still inconsistent.

I hypothesized that the difficulties might arise from the two areas that had always been problematic in the measurement process: integrating sphere corrections and lost light. The first problem could potentially be solved experimentally by

- determining the wall reflectivity of the integrating sphere,

- using smaller sample port diameters,

- using a reflectance standard whose reflectance was closer that of sample.

- making dual-beam measurements.

The second problem could presumably be solved by using larger samples. Little did I know.

Integrating sphere corrections

Integrating spheres are wonderful devices, but suffer from having a non-linear response to the presence of a sample. For example, even after correcting for dark noise, the detector on a sphere containing a sample with 25% reflectance will not measure exactly one-half the value of a 50% sample. (The presence of the sample changes the number of times that light bounces in the sphere. More reflective samples have more bounces and a greater chance of being captured by the detector. Thus the 50% sample will record slightly more than twice the value of the 25% sample. See figure 1).

Now `iad` has had code to account for the integrating sphere effect since the early 1990's. These corrections tended to be small and were easy to ignore. Moreover, the nomenclature we used was horribly obtuse *and* the derivation in the published papers contained minor errors [6]. This made it more or less impossible to use the integrating sphere correction factors unless one read the source code very carefully. Consequently, no one (including myself or my students) used it.

Instead of trying to find the errors in the earlier papers, my doctoral student Ted Moffitt and I re-derived all the necessary formulas. We used sensible nomenclature and I insisted that all the quantities have actual physical significance. I also eliminated unnecessary frills (e.g., baffles are now required). As a

consequence we came up with formulas that only required the experimentalist to know the various port sizes on the integrating sphere and the reflectance of the sphere walls. Incorporating these new formulas to the `iad` code also gave me the chance to develop a new input data file format. After forcing my students to use about twenty different versions, I finally came up with a file format that I liked. This new format forces the experimentalist to include all the relevant measurement parameters.

Unfortunately, despite a new file format and new sphere correction formulas, the optical properties of the phantoms were only consistent for the largest sample sizes (50 mm in diameter). This was good enough to finish the contract, but not really good enough to make me happy. I was confident that the experiments were performed correctly and I was equally sure that the light interactions with the spheres were correct. This indicated that the lost light was probably the source of any remaining discrepancies.

More recently, we now know that it is quite important to know the sphere wall reflectivity. For example on one sample the reduced scattering μ'_s increased from 1.66 to 1.91 mm^{-1} when the sphere reflectivity was changed from 0.960 to 0.973; consequently, it is important to measure the wall reflectivity of your spheres.

Version 3.0.0 — Solving the light loss problem

The light loss problem is simple. Light hits the front of a sample and the reflected light is collected by a sphere with a finite port size. Consequently, some light reflected by the sample will not collected (because it emerges on the reflection side outside the port). This light is lost. Furthermore, light collected by the sphere will uniformly and diffusely re-illuminate the sample. Some of this diffuse incident light will hit near the the edge of the sample port; when this light re-emerges from the front of the sample it will also have a chance of not being collected by the sphere.

The only way that I knew of to properly account for these two types of light loss was to use a Monte Carlo program. I refused to consider just swapping out the adding-doubling code and replacing it with Monte Carlo code. A few other groups have done exactly this, but I was stubborn. Monte Carlo programs are easily $10^4 \times$ slower than the adding-doubling method. I finally conceived of a hybrid approach that uses the inverse adding-doubling to quickly find the optical properties for a sample.

A Monte Carlo program is used to estimate the amount of light lost for this set of optical properties. This lost light is incorporated back into the next inverse adding-doubling estimate of the optical properties. This process is repeated until the optical properties stabilize. Most experimental situations only require a few Monte Carlo iterations before stabilizing. Furthermore, when analyzed with the new `iad` that accounted for lost light, all the earlier results for the contract phantoms that we made were now consistent!

User Issues 3

2   Installation

2.1   Obtaining the code

The source code is available as a `git` repository or as a zip archive of individual releases at

<https://github.com/scottprahl/iad>

The two distributions are `iad-3-16-2.zip` and `iad-win-3-16-2.zip`. The former contains the source files and the latter contains the same sources along with pre-built binaries `ad.exe` and `iad.exe` for Windows.

The original source files `foo.w` are written in CWEB, from which the source code files `foo.c` and `foo.h` files are generated. The documentation `foo.tex` is also generated from the same base `foo.w` files. This keeps the code and the documentation in one place and furthermore allows me to use the typesetting capabilities of TeX in the program comments (see `docs/ad_src.pdf` and `docs/iad_src.pdf`.

(The CWEB system really does produce beautiful documentation, but I do not think that offsets the fact that the code that is worth the hassles associated with debugging or the need to keep separate `.c` and `.h` versions in sync with the distributions.)

2.1.1   Building

This code has been compiled and tested on a variety of unix computers (MacOS X PPC, MacOS X Intel, Red Hat Linux x86, and SUSE Linux x86) and microprocessors (PPC, x86, and Arm (Raspberry Pi and Apple M-Series).

To compile an executable

```
prompt> unzip iad-3-16-2.zip
prompt> cd iad-3-16-2
prompt> make
```

This should produce two executable files `ad` and `iad`.[5]

2.1.2   Testing

Once the code has been compiled, `iad` can be tested by running

```
prompt> make veryshorttest
```

A more extensive set of command-line tests can be run using

```
prompt> make test
```

Finally, if you want to run tests against various datasets in the `test` directory, then do

```
prompt> make longtest
```

---

[5]To recreate all the files from the originals you'll need `perl`, pdfLaTeX, `cweb` and `gindent`.

3   Experimental Decisions

OK, now you need to decide how you will actually make the measurements. The table below relates the basic premise that you can't get something for nothing; it gives the necessary measurements for a particular of optical properties.

Optical Property	Measured Values	Comments
μ_a	M_R	The sample thickness is assumed to be too thick to get any light through. To estimate μ_a, the anisotropy is fixed (default $g = 0$), and $\mu_s = 1/\text{mm}$.
μ_a, μ_s'	M_R, M_T, δ	The anisotropy is fixed (default $g = 0$).
μ_a, μ_s, g	M_R, M_T, M_C, δ	Three measurements are made.

3.1   Decisions that you do not have to make

The `iad` code is quite flexible. In the initial releases, I thought that it was important to expose all this functionality. This had the unfortunate side effect of making easy things hard. This release is intended to make the easy things easy and while hard things remain possible (you can write your own code that calls the subroutines in `iad`).

> I have made a bunch of decisions for you.

For example, the `iad` requires that the *total* reflection M_R and *total* transmission M_T be measured. You did not need to decide if the unscattered reflection or unscattered transmission should be included. Sometimes people like to bounce the specular reflection of the glass slide out of the entrance port (or into a beam block) so that their diffuse reflection measurement will be cleaner. Alternatively, some people like to allow the unscattered transmitted light to leave the sphere so that their diffuse transmittance measurement will be better. I decided that, in general, both of these are bad ideas.

My rationale was that experimentally separating the unscattered light from the slightly scattered light is difficult. Handling the unscattered light in the program is trivial, estimating the loss of scattered light accurately is hopeless. In the reflectance case, the specular beam reflected from the sample must travel a good distance before exiting the sphere. Ideally, this light would be a nice laser beam that would not diverge appreciably. Unfortunately, illumination is nearly alwyas a white light source and an indefinite fraction of light will be lost out the port by which the unscattered light leaves. (Similar arguments hold for the transmitted light, with the additional caveat that the transmitted light that is only scattered a few times is strongly directional and therefore constitutes another unknown.)

Another decision I have made is how you must measure M_R and M_T. If you look at figure 3, then it seems like a pretty reasonable set of measurements. However, we tried a couple of other schemes, like making $R(0,0)$ more like an R_{dark} experiment, i.e., just block the illumination beam. The problem with this method is that usually one does not have a small, tight illumination beam and therefore there is usually a non-negligible amount of light that misses the sample and hits the sphere walls directly, $R(0,0) > 0$. A similar situation exists for the transmission sphere, but because the light never enters the sphere, the background problem is much smaller.[6]

I have also selected the experimental parameters needed in the header of the data files. You are forced to enter these values for every experiment that you analyze. These are parameters that I, and hopefully you, will readily comprehend. For example, the header used to contain the value of a_s, but I could not look at the file header and know what the sphere size was. Similarly, instead of the easily understandable detector diameter, a weird b_2 factor was used because it made things a little simpler for the code.

I have also decided that you must always have a baffle between the sample and the detector. As I said before, it is just too hard to estimate the amount of light that directly reaches the detector on the first bounce.

3.2   Which reflectance standard?

You will need some reflectance standards for the reflection measurement. Common NIST (no longer NBS) traceable standards are obtainable from LabSphere. I suggest buying from Avian Technologies[7] If you have little money, but lots of time, then you can make your own spheres and plates. These should be freshly coated with magnesium oxide (MgO) or you can use barium sulfate (BaSO$_4$). Both coatings are somewhat fragile and the MgO coating has poor reflectance in the blue and UV region.

One thing that is not obvious is what value of reflectance for the standard is most desirable. It is important that the reflectance standard have higher reflectance than your sample.[8] The background reflection (nothing in the sample port) establishes the lowest amount of light reflected by a sample. The maximum amount of light should occur when 100% of the light is reflected by the sample. When such a standard is used, then all the sample measurements will fall between these two extremes (0% and 100%).

Unfortunately integrating spheres do not have a linear response to different sample reflectances (see Figure 1). This graph shows that the corrections needed for the sphere are least at the two ends, and highest in the center. The

---

[6]Using a two glass slides surrounding air or water sounds like a plausible 100% transmission (or 0% reflection) experiment. Unfortunately, interference within the slides leads to disturbingly large variations in this important reference experiment. Try it, you will be surprised how variable your results can be.

[7]http://www.aviantechnologies.com

[8]It is axiomatic that you want to interpolate your measurements between two known points rather than extrapolate past them.
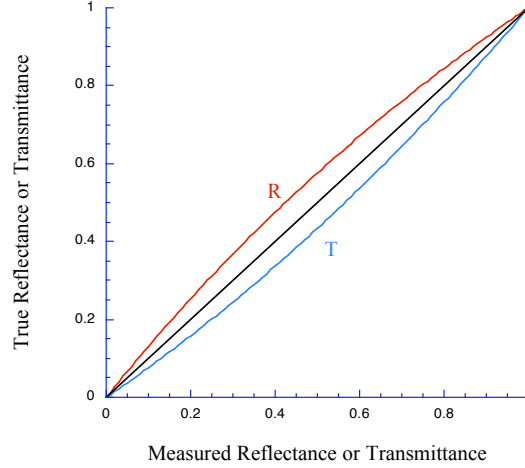
Figure 1: The relationship between measured values using an integrating sphere and the true values. In this graph, it is assumed that the dark measurement was completely dark and that the reflectance standard was 100%. These effects are typical for a relatively large sample port (50 mm port) in a moderate size integrating sphere (200 mm diameter). In general the measured values using an integrating sphere will tend to underestimate reflectance measurements ($M_R < R$) and overestimate transmittance ($M_T > T$).

corrections needed for the center depend on the geometric size of the sphere and ports as well as on the sphere wall reflectance. To minimize the need for these corrections, it is best to use a reflectance standard that is slightly higher than all the sample reflectances. This will reduce the magnitude of the sphere corrections and therefore the sensitivity of your measurement to integrating sphere parameters.

The magnitude of the sphere correction can be huge. For example, we were making measurements[9] on non-scattering, dark polyurethane samples using the substitution (single-beam) method. Now, the index of refraction of polyurethane is ~1.5 and therefore the reflectance of the sample will be at least 4% due to specular reflectance. However, our measurements were consistently giving us 3%. The ultimate reason was that the sphere efficiency (gain) was so much greater for the standard reflectance measurement than it was for the sample reflectance measurement that when calculating M_R it came out 25% lower than expected. Obviously, this effect would have been mitigated if we had followed

---

[9]Hi Beatriz!

my own advice and used a dark reflectance standard, but I am sure that I had a good reason for ignoring myself.

3.3 Which integrating sphere?

There is a long history of the use of integrating spheres [5, 112–116]. Good 'ole Ulbricht proposed the first one a hundred years ago [113]. You can make your own easily. Just get a sphere, e.g., a child's ball and cut it in half. Paint the inside with $BaSO_4$, glue it back together attach detectors and voilá! Or you can plunk down a thousand bucks and buy one from LabSphere.

The integrating sphere is characterized by its diameter, its ports, its baffle, and its wall reflectance (typically ∼98%). In all the discussion and code that follows, it is assumed that the baffle (inside the sphere) is located between the sample and the detector. This ensures that all the light leaving the sample hits the diffuse white coating on the sphere walls and is more-or-less uniformly distributed across the sphere walls. If the baffle is not present, then some (unknown) fraction of light directly propagates from the sample to the detector, while the rest of the light bounces around in the sphere. It is possible approximate the light captured by the detector and sample, but this depends on the extent of the emission profile from the sample, the geometry between the sample and the detector, as well as on the reflectance of the detector at that angle. It is much better just to require the presence of a baffle and avoid the whole mess.

The size of the sphere is usually determined by what sphere you happen to have in the lab. The sphere diameter pretty much determines the maximum sample port size. The theory of integrating spheres assumes that the sphere is spherical in shape. Obviously if you create a port in the sphere by slicing off a large chunk of the sphere and then place a flat sample on of the sample port you will no longer have a perfect sphere. A rule of thumb is that you do not want the sample area to be more than 10% of the sphere wall area.

The size of the sphere dictates the largest sample size, but the illumination beam determines the smallest sample size. Ideally the entire beam would hit the sample. In a transmittance experiment, light that misses the sample is a disaster because that light is difficult to properly measure experimentally.[10] Light that misses the sample in a reflectance measurement is less problematic. That light should be properly accounted for by the calibration measurements, but the light that misses the sample significantly adds to the background noise in the reflectance measurement.

The sample size is also connected to the sample thickness. Generally, one wants to have large aspect ratios for the sample (port diameter is ten times

---

[10]One might argue that the light does not enter the sphere at all and therefore will be properly accounted for by the calibration measurements. This is true, but (1) the calibration measurements will be exquisitely sensitive to shifts in the beam profile, (2) you are throwing away some signal immediately, and (3) by illuminating with a beam that is equal to the entrance aperture, you are maximizing losses out the edge of the sample—these are accounted for by `iad`, but will cause `iad` to run much more slowly because multiple attempts will be needed to properly calculate the light losses.

the sample thickness.) So for example, a beam $1\,\mathrm{mm}$ in diameter, a sample $1\,\mathrm{mm}$ thick, a port $10\,\mathrm{mm}$ in diameter, and a sphere $100\,\mathrm{mm}$ in diameter are all reasonable, practical values.

3.4 How many spheres?

This seems simple right? Why have a whole section devoted to counting the number of spheres? Well, mostly because the program treats the cases of 0, 1, and 2 spheres differently. The `iad` program always reads the same number of sphere parameters at the beginning of each data file (i.e., from the header). Therefore, even if you specify zero spheres, you will need to include values for two spheres in every data file.[11]

3.4.1 Zero

When you specify 0 spheres, then the program assumes that you have made measurements of the sample in such a way that the values that you specify for M_R and M_T are devoid of integrating sphere errors and therefore `iad` *makes no corrections for the integrating spheres.* Good reasons for choosing this are

- You just want to get a quick estimate and can't be bothered to type in the five parameters needed to characterize the sphere (even though I made it really, really, easy for you.)

- You are making your measurements using the comparison method (dual beam) *and* you don't think that the uncollected light from the initial direct illumination is significant.

- You want to evaluate how much an effect the sphere corrections are having on your final derived optical properties.[12]

- You don't know the sphere wall reflectivity. If you want to have robust measurements then there is some merit in determining the reflectivity as outlined in this document. This measurement is consistent with the basic assumptions made in the program and helps to eliminate some sorts of systematic errors.

3.4.2 One

When you specify 1 sphere, then a single sphere is assumed to have been used to measure the sample reflectance and transmittance. This does not have to be the same sphere, but it is assumed that a second sphere is not present in a way that

---

[11]Insane, I know, but the original `iad` did not require this, and automated processing became tricky. It was surprisingly hard to maintain the code and unnecessarily confusing. Now I figure that it is easier for me to make you copy-and-paste sphere parameters than it is for me to continually update `iad`.

[12]There is a simpler way to do this, just specify `-s` as a command line switch when processing your data.

it affects the results of the sphere making the measurements. *The program will use the values in the header to make corrections for a single sphere.* The values for the reflection sphere and the transmission sphere do not need to be identical — a single sphere means that one sphere is used at a time for all measurements.

3.4.3 Two

Using two spheres is actually why I was originally interested in this problem.[13] There are a few good reasons to use two spheres. First, if the sample is has dynamically changing optical properties, then it is critical that both M_R and M_T be measured at the same time. Another reason might be that you would like to measure the greatest number of samples in the shortest possible time.

Nevertheless, there are a couple of drawbacks to using two spheres at once. The first drawback is the prosaic problem of making good contact on both sides of the samples with the spheres.[14] One does not want to squish one side of the sample so that just barely adequate optical contact is reached on both sides. The second drawback is that it is a pain in the neck to make the calibration experiments.

3.5 What about dual-beam spectrometers?

Dual-beam spectrometers use two beams: the sample is placed in one beam and a reference is placed in the second beam. Two measurements are made (usually sequentially) and the reference beam is used to correct for system effects like lamp variation with wavelength or detector changes or anything that affects the light path. For example, two cuvettes might be used with one cuvette being a reference that allows most of the effects of specular reflection from surfaces to be corrected. We are most interested when two beams are used in an integrating sphere. The two common beam geometries are shown below
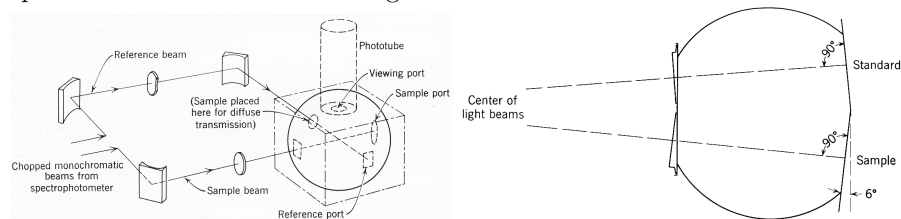
in these two (modified) images [117]. In both these examples the beam is incident perpendicular to the samples, but the angle between the beams might be ninety degrees (left) or shallow (twelve degrees on the right).

So why do I, or actually you, care? The geometry implies a different method of normalization. The good part is that "sphere corrections" are not needed any

---

[13]Back in the day, laser heating and coagulation of tissue was *the* application of interest. Since no one knew how the optical properties changed during high power irradiation, I tried to measure the changes in optical properties as they changed.

[14]One of our spheres was dropped and one port is not parallel to the port on the opposite face. Since the internal light baffles pretty much determine the necessary sphere orientation, this makes double integrating sphere measurements tricky.

longer. Because both the reference and the sample are present in the sphere during reference and sample measurements, the sphere efficiency remains constant and no "sphere corrections are needed."

Light losses are another issue. The direct light loss is completely unaccounted for in the dual-beam sphere. Oddly, the diffuse light loss *is* properly accounted for because the diffuse sample reflectance only enters into the calculation when figuring out the integrating sphere efficiency. Since the sphere efficiency for the sample illumination and the standard illumination are equal, the diffuse light loss is not an issue.

Anyhow, if you are using a dual beam system, then if your system automatically gives you the ratio of the sample reflectance to the standard reflectance, you will want to calculate M_R

$$M_R = r_{std}(R_s - R_0)$$

where R_0 is a measurement obtained with nothing in the sample reflection port and is present to correct for light that misses the sample and hits the sphere wall first. The value for M_T is similar

$$M_T = t_{std}(T_s - T_0)$$

although now T_0 is made with a blocked sample port and represents the least amount of light that may be measured.

How does one analyze these in practice with IAD? Well, the simplest way is to just to use the `-X` option[15] and specify the sphere parameters that you used.

3.6   How should the sample be prepared?

There are a whole host of experimental problems which plague measurements of reflectance and transmittance. Inattention to experimental details will yield garbage. Just look at the variation in the optical properties gathered together in Cheong *et al.* [4]. These can be attributed to two sources of error—inattention to the details of the experimental measurement and to flaky optical models. Since presumably, the adding-doubling method is *not* flaky, you are saved from the second source of error. But I can do nothing about saving you from poor experimental technique except to warn you about various things.

3.6.1   Freshness

If the sample is not fresh then optical properties will differ from those measured *in vivo*. Obviously, the tissue begins rotting as soon as its nutrient supply is removed. If the tissue is not in excellent condition then there will be problems. By the way, there has been essentially no work done on the changes in optical properties which take place when a tissue is removed. There has been minor work done on the changes in optical properties with heating, but nothing to that definitively says that the optical properties measured *ex vivo* are even close to those *in vitro*.

---

[15] The 'X' is for crossed beams.

3.6.2 Boundaries

The need for glass or quartz slides at the boundaries is caused by the rough surface of most tissues. Since the boundaries are characterized by Fresnel reflection, it is relatively important for the experiment to match the quantities calculated by the code. Water, saline, or best phosphate buffered saline (PBS) or some other fluid should be used to ensure good index matching between the tissue and the slide. Care should be taken to ensure that no bubbles are formed between the slide and the tissue. Since the index of refraction of glass is 1.5 and that of tissue ranges from 1.33 to say 1.45, the boundaries are not perfectly matched. You just have to live with this or experiment with various immersion oils and various glasses and plastics achieve perfection.

3.6.3 Hydration

Optical properties of the sample definitely change with the amount of water in the tissue. It is important to store the tissue in air-tight containers sandwiched between moist (with PBS) towels at cool (above freezing) temperatures. If you don't believe me, then leave a piece of tissue exposed to air for 48 hours. It will appear quite different from fresh tissue.[16] Since your eye sees reflected and transmitted light, any measurements will also differ.

3.6.4 Sample Diameter

How big should the sample be? First, it must be larger than the sample port in the integrating sphere. If not, then make the port smaller. Second, you want the distance from the edge of the irradiating beam on the sample to the edge of the port (h) to be as large as practicable. If,

$$h \gg \frac{1}{\mu_a + \mu_s'}$$

then relatively little light will be lost out the sides of the sample. "Relatively little" is a complex and depends on other things. In general, it is hard to predict without modelling carefully. Before the Monte Carlo correction was added to this code, all losses would be attributed to absorption. Consequently, any absorption coefficients generated for this sample will be too large. The ramifications now are less dire: lost light takes longer to analyze because the amount of lost light must be continually recalculated.

3.6.5 Variability

From spot to spot on one sample and from sample to sample. Make enough measurements that you have some idea of the average value and variance for each sample as well as the variability from sample to sample.

---

[16]Your co-workers will probably complain bitterly about the smell, but we are only concerned about the appearance of the tissue.

3.6.6   Blood

Should samples be measured with or without blood? Clearly neither really is a good example of the in vivo situation. If samples have no blood then the optical properties of the sample itself are being measured. The contribution to blood can be added later.

3.6.7   Freezing

To obtain very thin subsections it is necessary to freeze the sample. Rumor has it that the freezing process changes the optical properties. The evidence for this has been on muscle tissue. Other tissues like aorta and dermis are different and not so susceptible to freezing artifact.

3.6.8   Interference

Serious pain in the wahzoo. The interference usually comes from multiple internal reflections from the glass slides which sandwich the tissue sample. When a laser beam strikes the air-glass surface it is reflected. It is also reflected at the glass-tissue surface. This reflectance can interfere with the first reflectance. One would expect this to be a neglible effect, but in practice it can nearly 10%. It is easily demonstated by placing a microscope slide in the path of a laser beam and measuring the transmission. Then move the slide slightly and observe the transmission again. An even more dramatic effect is achieved when specular reflectance is measured.

What can be done? Sit down with a box of microscope slides and go through them one by one observing the reflectance profiles on a wall. Discard all those that show definite interference effects. These should be the least optically flat of the whole box.

Another possibility is to use very thick glass plates. By slightly rotating the plate the reflectance from the second surface will be displaced sufficiently that the two beams will no longer be aligned and consequenly will not interfere. Thick plates are not ideal because they displace the integrating spheres and consequently all some diffuse light to be lost before it can enter the integrating sphere.

A final posibility is to use optically flat plates. Interference will be constant over the surface and can be measured and accounted for. This is the best option, but also the most expensive.

4 Measurements

4.1 Integrating sphere calibration

The sphere wall reflectance r_w is critical. Hopefully, you have a new, well-maintained sphere whose manufacturer-specified value for r_w is accurate. Measuring the wall reflectance r_w is challenging, but can be done. Two measurements are needed (figure 2),

$$\frac{1}{r_w} = a_w + a_d r_d (1 - a_e) + a_s r_{std} (1 - a_e) \frac{R_{std}^{diffuse}}{R_{std}^{diffuse} - R_{0}^{diffuse}}. \tag{1}$$

This equation illustrates the difficulty in making accurate measurements of the sphere wall reflectance. The two diffuse reflectances $R_{std}^{diffuse}$ and $R_{0}^{diffuse}$ will only differ by the amount of diffuse light leaking from the sphere when the port is empty. Consequently the difference will be small and any errors in the measurements will be magnified when the division is done.
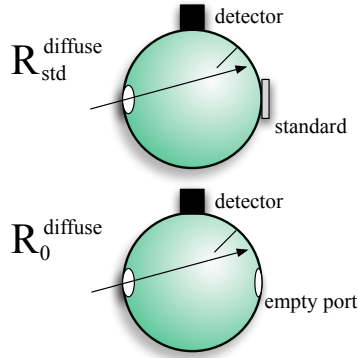
Figure 2: The two experiments needed to determine the sphere wall reflectance. The reason that this is a hard experiment to do well is that the quantity of interest is the difference between the two measurements. This is a small difference and is roughly proportional to the relative area of the sample port a_s.

4.2   Single Sphere M_R and M_T

Standard usage is that *reflection* is the light being reflected by the sample, while the *reflectance* is the light being reflected by the sample normalized by the incoming light. Reflectance has no units. A stable useful estimate for the reflectance of the sample is the *measured total reflectance M_R* which is defined in terms of easily measurable sample, standard, and background reflection measurements:

$$M_R \equiv r_{std} \cdot \frac{R(r_s^{direct}, r_s) - R(0,0)}{R(r_{std}, r_{std}) - R(0,0)}. \tag{2}$$

where $R(r_s^{direct}, r_s)$, $R(0,0)$, and $R(r_{std}, r_{std})$ are defined in Figure 3.[17]

The same idea applies to *transmission* and *transmittance*; the transmission has units while the transmittance is normalized to the incident power. The *measured total transmittance M_T* is defined as

$$M_T \equiv \frac{T(t_s^{direct}, r_s) - T_{dark}}{T(0,0) - T_{dark}} \tag{3}$$

where $T(t_s^{direct}, r_s)$, $T(0,0)$, and T_{dark} are defined in Figure 3.

---

[17]The value of M_R differs from the true reflectance because the gain of the integrating sphere varies with the sample reflectance (see Figure 1).
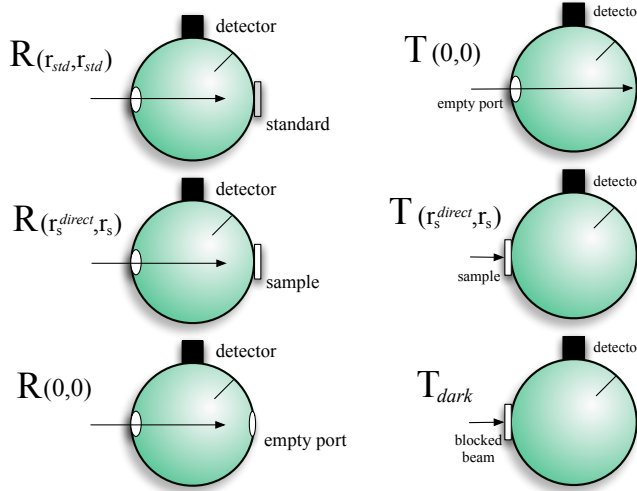
Figure 3: The measurements needed to measure M_R and M_T in equations 2 and 3. Note that the baffle is always located between the sample and the detector. The back wall of the transmission sphere is never open (light that does not interact with the sample bounces around in the sphere). Finally, notice that T_{dark} and $T(0,0)$ are very different.

4.3   Double Sphere M_R and M_T

Double sphere values for M_R and M_T differ slightly from that for single spheres. The experimental arrangement for the spheres in double-sphere measurements is shown in Figure 4. The normalized reflectance is then

$$M_R = r_{std} \cdot \frac{R_2(r_s^{direct}, r_s, t_s^{direct}, t_s) - R_2(0,0,0,0)}{R_2(r_{std}, r_{std}, 0, 0) - R_2(0,0,0,0)} \tag{4}$$

and transmittance by

$$M_T = \frac{T_2(r_s^{direct}, r_s, t_s^{direct}, t_s) - T_2(0,0,0,0)}{T_2(0,0,1,1) - T_2(0,0,0,0)}. \tag{5}$$
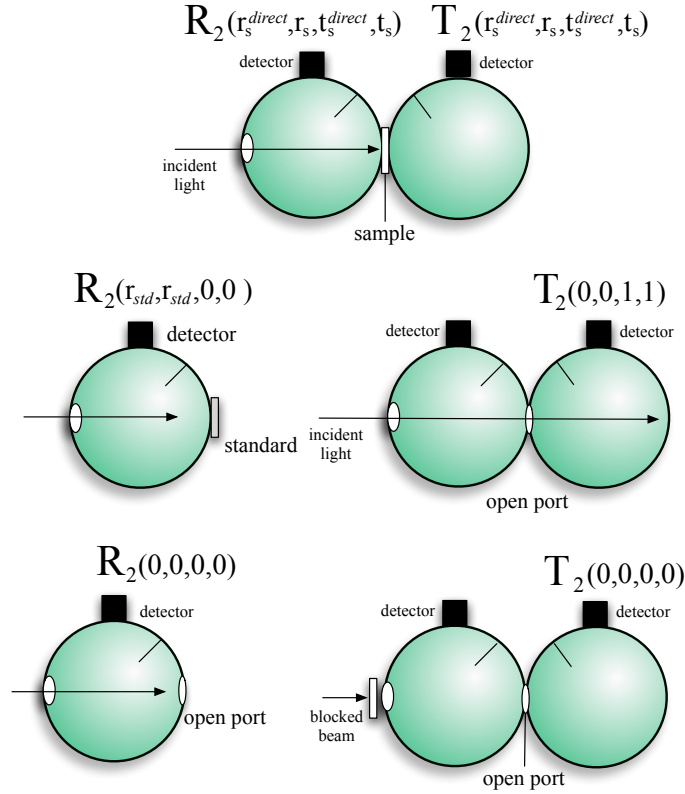
Figure 4: Measurements needed for M_R and M_T when two integrating spheres are used simultaneously.

4.4 Measured Unscattered Transmittance

Finally, the *measured unscattered transmittance* M_U is the amount of light that gets through the sample without being scattered or absorbed. This has been called by a bunch of different terms: collimated transmittance, ballistic transmittance, on-axis transmittance, coherent transmittance.

$$M_U \equiv \frac{U_s - U_0}{U_{100} - U_0} \tag{6}$$

where U indicated an unscattered measurement. In this equation, U_s refers to the unscattered sample transmission, U_0 is the background measurement for the unscattered transmission measurement (beam blocked) and U_{100} is the unscattered transmission measurement when no sample is present.
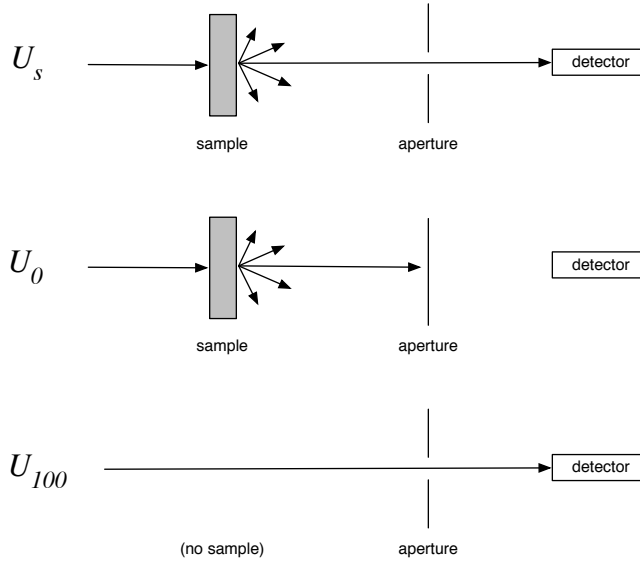
Figure 5: Measurements needed to determine M_U.

The measured unscattered transmittance is the most difficult measurement to make and it is frequently underestimated how hard it is to get correct. Be careful. Do yourself a favor and plot your measured values for unscattered transmittance versus the concentration or sample thickness. If this line is not exponentially decreasing then you have problems. Furthermore, you should check to make sure that your data passes through the correct value when concentration or sample thickness is zero. This is easily calculated using the indicies of refraction. For example, for water ($n = 1.33$) between glass slides ($n = 1.50$) the transmittance should be roughly

$$M_U = (0.96)(0.996)(0.996)(0.96) = 0.914$$

where I have neglected to include multiple internal reflectances. The `iad` program does, but then it is good at that sort of thing.

Next, do a quick calculation to ensure that the amount of *scattered light* reaching the detector is significantly less than the estimated value for the unscattered transmittance. Since

$$M_U \propto e^{-(\mu_a+\mu_s)\delta}$$

the value for M_U gets small, very quickly! Do not underestimate the enormity of the smallness of M_U! Remember, if your collimated transmittance data does not pass the above test, then the output from the `iad` program must be suspect. *Garbage in, garbage out.* It is undoubtedly better to assume a value for the anisotropy than to use a flawed value for the unscattered transmittance.

For scattering samples, measurement of unscattered transmittance is more complicated because any transmission measurement consists of contributions from both unscattered and scattered light.

$$U_{measured} = U_{scattered} + U_s$$

I can think of at least three methods for finessing this problem.[18] Reasonably accurate values for the measured unscattered transmittance can be obtained by make measurements at (1) various distances, (2) various angles, (3) with very thin samples in which the contribution from scattering is negligible. The last two methods are described in the paper by Jacques, Alter, and Prahl [118]. The other method has not been published (as far as I know—since I thought it up and have not had the time to go to all the trouble to write it up and review the literature.)[19]

If the light incident is perfectly collimated (no divergence) and the scattered light is isotropically distributed over all angles,[20] then the amount of light dectected at a distance z from the sample is

Measured Power [W]		Scattered Intensity [W sr^{-1}]	×	Detector Solid Angle [sr]	+	Collimated Irradiance [W cm^{-2}]	×	Detector Area [cm^2]
	=							

where the solid angle subtended by the detector located at a distance z from the sample is

$$\text{detector solid angle} = \frac{\text{area of detector}}{\text{area of sphere with radius } z}$$

If the scattered light exiting from the back of the sample is isotropic then the intensity for this light will have a constant value I_{scat}. Therefore, if the

---

[18]Aside from using optical coherence tomography (OCT) or time-of-flight measurements

[19]I should probably mention that polarization can also be used to increase the collimated to scattered ratio. Unfortunately this only attenuates the diffuse contribution by a factor of two for thick samples (whose diffuse transmittance will be unpolarized.)

[20]This is a surprisingly good approximation when more than two scattering events take place in the sample.

irradiance is E_0 then the unscattered transmission measurement will be

$$U_{measured} = \frac{I_{scattered}}{4\pi z^2} + U_s$$

Notice that the first term (the scattered light) decreases with the sample detector separation z. For a perfectly collimated beam U_s will be independent of the distance z, and therefore the first scattered term may be made as small as desired by moving the sample farther and farther from the sample. U_s is the limit of as the separation between sample and detector becomes infinite. Thus, if $U_{measured}$ is known for several distances between sample and detector, linear regression might yield both U_s and the scattered intensity.[21]

---

[21]A major assumption in this development is that the scattered light exiting the sample is isotropic. This is true for optically thick samples but definitely not for optically thin ones [118].

5 The Data File

The basic structure of the data file consists of a header section followed by your measurements of reflectance and transmittance. The header describes details of the experiment: the sample thickness, the beam diameter, the indices of refraction, the number and geometry of the spheres used.[22]

5.1 The header

The header was designed to be

1. easily annotated for humans
2. sufficiently flexible to accommodate all common experiments
3. readily parsed by machine
4. filled with entries that have a simple physical meaning
5. a complete description of experimental geometry
6. devoid of rarely-used parameters

These goals were achieved by carefully specifying a minimal set of parameters that describe a particular experiment and developing a simple comment style. At its simplest, the header consists of the identifying tag `IAD1` followed by eighteen numbers.

The first four characters of the file must be `IAD1`. This allows the program to do basic sanity checking of the file before beginning to parse the file. The final digit may one day be used as a version number. I hope not. Anyway, one example of a valid header is the sequence `IAD1` followed by 18 numbers,

```
IAD1 1.34 1.5 1 1 5 .96 1 203.2 25.4 12.7 1 .96 203.2 25.4 12.7 1 .96 2
```

This short example is functionally identical to the longer annotated example that is shown below. Of course, this version is not suitable for human consumption. Nevertheless, it demonstrates that (1) the comments help readability tremendously, (2) the quantity of the parameters is fixed, and (3) the ordering is fixed.

To make my life easier, I allow and nearly always use comments. A number sign (#), aka octothorpe, pounds sign, or hash symbol is used to start a comment; everything from the number sign to the end of the line will be ignored. White space and comments are ignored except when following a number. There is no difference between comments, tabs, spaces, linefeeds, or carriage returns; any one will end a number.

---

[22]Details about *how the measurements should be analyzed* are handled by command-line options (next section). This allows one (for example) to assume different default anisotropies, a different number of quadrature points, or different constraints on the Monte Carlo simulations. Of course, this is also a lie. I have extended the number of command-line parameters to allow one to specify all the parameters in the header of the data file. This allows one to do an IAD calculation without needing to create an input data file, which I find to be useful when scripting tasks — or asking *what if* questions from the command-line.

```
IAD1   # Must be first four characters

# Input Example with a single set of sphere coefficients
# The order of entries is important
# Anything after a '#' is ignored, blank lines are also ignored

1.34   # Index of refraction of the sample
1.50   # Index of refraction of the top and bottom slides
1.0    # [mm] Thickness of sample
1.0    # [mm] Thickness of slides
5.0    # [mm] Diameter of illumination beam
0.96   # Reflectance of the calibration standard

1      # Number of spheres used during each measurement

       # Properties of sphere used for reflectance measurements
203.2  # [mm] Sphere Diameter  (8 in * 25.4 mm/in)
25.4   # [mm] Sample Port Diameter
12.7   # [mm] Entrance Port Diameter
1.00   # [mm] Detector Port Diameter
0.96   # Reflectance of the sphere wall

       # Properties of sphere used for transmittance measurements
203.2  # [mm] Sphere Diameter  (8 in * 25.4 mm/in)
25.4   # [mm] Sample Port Diameter
0.00   # [mm] Entrance Port Diameter
1.00   # [mm] Detector Port Diameter
0.96   # Reflectance of the sphere wall

2      # Number of measurements, M_R, M_T
```

In this annotated header, the details of the geometry of the experiment are immediately apparent: reflectance and transmittance was measured using a single sphere in which the 12.7 mm diameter sample was illuminated by a 5 mm diameter beam. We also know that the sample was sandwiched between glass slides ($n = 1.5$) that were 1 mm thick.

The last number in the header determines how many measurements are available. This number may vary from 1 to 6 depending on the experimental circumstances.

When using one reflectance sphere, the entrance port diameter defined as the size of the port though which light enters the sphere. The sample port is the size of the hole in the sphere that is adjacent to the sample.[1] Finally, the detector port diameter is the size of the port that houses the detector or optical fiber that goes to the detector. The reflectivity of all the ports is assumed to be zero — i.e., the ports are black.

If your detector is not round, but rectangular, then the detector diameter should be chosen to match the area of your detector. Thus if your detector is a rectangle $10 \times 1 \, \text{mm}^2$, you would use a diameter of $\sqrt{40/\pi} \approx 3.6 \, \text{mm}$. Furthermore, if you have multiple detectors in your sphere (e.g., for different wavelength regions), the detector diameter should correspond to area equal to the sum of all the detector areas.

When using one transmission sphere, the entrance port should be set to zero. We are assuming direct collimated illumination of the sample. The sample port

---

[1]The actual sample size is always assumed to be larger than the sample port. In fact, the sample is assumed to have infinite lateral extent. It is a challenge when working with small pieces of tissue to maintain a large port size and still have the sample port completely covered by the sample.

size should be set to the size of the port next to the sample. The detector size should be set as described above. The reflectance and transmittance spheres differ in the number of places that light can be lost. A reflectance sphere loses light out the entrance port, the detector port, and the sample port (through the sample). A transmittance sphere loses light only from through the detector ports and the sample port.[1]

5.2   The data section

After the header comes measurements of the reflectance M_R and transmittance M_T. This is sort of a wonky section because I wanted to have a reasonable amount of flexibility; this especially handy when combined with unix scripting to automatically process large numbers of integrating sphere measurement files. The organization is not *that* confusing, but you should read this section to understand why things are the way they are. My rationale will not make the layout any less kludgy, but it may provide a modicum of amusement where otherwise there would only be anger and frustration.

Ideally one would always have three (or more) measurements. Unfortunately, often the unscattered transmittance measurement is not available. For example the the amount of unscattered light that propagates through a millimeter of tissue is very small. For thicker samples the total transmitted light M_T is zero also. In this case then only one parameter can be measured. The following describes how you deal with multiple columns of data.

5.2.1   White space

The same rules for white space and comments that apply in the header section also apply to the data section. This means that you can liberally comment your data (or not) by using `#` to start a comment.

5.2.2   Optional wavelength entry

The `iad` program is mainly intended to analyze spectral measurements of reflectance and transmittance. For a number of reasons (e.g., graphing) it is convenient to precede the measured values by the appropriate wavelength,

```
#lambda   M_R       M_T
   800    0.16830  0.24974
   810    0.16271  0.26479
   820    0.16289  0.25530
```

Since we don't want to require wavelength data, it would be nice if `iad` should also give identical results for input data like this

---

[1]Of course, in our current set up in the lab, we have mounted the reflectance fiber permanently in one sphere that is used for both transmittance and reflectance measurements. In this case, there are identical causes of light loss in both spheres and therefore the entrance port size in the transmittance sphere might be non-zero or this area could be lumped into the detector port size. In practice it is just easiest to make the parameters for both spheres be equal to one another.

```
# M_R      M_T
0.16830  0.24974
0.16271  0.26479
0.16289  0.25530
```

There are at least two possible solutions to solve this problem: add another parameter to the header or auto-recognize the presence of a wavelength. Since I wanted to keep the number of parameters in the header to a minimum, I went with the second option. This leads to the following rule.

If the first number on a line is greater than one, that number is assumed to be a wavelength, otherwise it is interpreted as M_R.

The value of the wavelength is not used anywhere except for being copied to the output file. The above rule means that you cannot measure your wavelength in microns if that forces the wavelength to fall between 0 and 1. For example 532.8 is fine as a wavelength but 0.5328 will be interpreted as a value for M_R. This is why all the example files in the test directory use nanometers for the wavelength range.

5.2.3 One measurement

```
#lambda   M_R
  800      0.16830
  810      0.16271
  820      0.16289
```

When the only measurement specified, it is assumed to be the measured reflectance M_R. Since there is only a single measurement two assumptions are made:

- the optical thickness of the slab is assumed infinite and

- the anisotropy coefficient set to the default value ($g = 0$ unless a specific command-line value has been specified).

The albedo is varied until the correct value for the measured reflectance M_R is obtained. Now `iad` generates both absorption and scattering coefficients. Because only the albedo is known, and `iad` reports both the scattering and absorption, some value for the scattering coefficient is assumed ($\mu_s = 1$). There is really no good reason for this other than the general observation that scattering is relatively constant (as a function of wavelength) for most samples that are measured. One might process a reflectance-only data set to get a sense of how absorption varied across the range of input values.

More recently, I have expanded the command-line options for `iad`. This means that if you happen to know the absorption coefficient and have a reflectance measurement you might try

```
prompt> iad -A 0.01 -g 0.6 file.rxt
```

which will constrain the $\mu_a = 0.01\,\mathrm{mm}^{-1}$ and the $g = 0.6$. Therefore the scattering coefficient will be found.

5.2.4   Two measurements

```
#lambda   M_R      M_T
  800     0.16830  0.24974
  810     0.16271  0.00000  #treated as one measurement
  820     0.16289  0.25530
```

This is the most common case and

- the anisotropy coefficient set to the default value ($g = 0$ unless a specific command-line value has been specified).

The first two values are the measured reflectance and the measured transmittance. As long as $M_T \neq 0$ then the anisotropy coefficient set to the default value and the albedo and optical depth are varied until the correct values of M_R and M_T are obtained. The scattering and absorption coefficients are calculated from the final values for the albedo and optical depth and printed. When $M_T = 0$ then the situation is identical to the one measurement case above and is treated in exactly the same way.

5.2.5   Three or more measurements

```
#lambda   M_R      M_T      M_U
  800     0.16830  0.24974  0.0012
  810     0.16271  0.00000  0.0000 #treated as one measurement
  820     0.16289  0.25530  0.0000 #treated as two measurements
```

If both $M_T \neq 0$ and $M_U \neq 0$, then M_U is used to calculate the optical thickness directly. The optical thickness is calculated by including all the multiple internal reflections in the slide and sample and using M_U. The albedo and anisotropy are varied until M_R and M_T are matched.

If $M_U = 0$ but $M_T \neq 0$, then the situation is identical to the two measurement case above. Finally when both $M_T = 0$ and $M_U = 0$ then the single measurement case above applies.

5.2.6   Four measurements

```
#lambda   M_R      M_T      M_U      r_w
  800     0.16830  0.24974  0.0012   0.951
  810     0.16271  0.00000  0.0000   0.952 #treated as one measurement
  820     0.16289  0.25530  0.0000   0.953 #treated as two measurements
```

This is how `iad` handles the situation in which the sphere wall reflectance varies with each measurement (e.g., as a function of wavelength). Both the reflectance sphere and the transmittance sphere wall reflectances are changed by this value. If you want to use this option when you only have one or two measurements, then indicate that you have four measurements and enter 0.00 for the unknown values (as in the 810 nm line above). This option was originally needed because we needed to use a sphere that was coated for use in the visible with wavelengths from 1,000–1,600 nm. In this region the wall reflectance changed significantly over the wavelength range that we were using.

The real advantage of including the sphere wall reflectance measurements r_w that were made according to section 4.1 are that it negates a variety of systematic errors that might be present in your measurement. Since the r_w

measurement is made with the same light source, detector, spheres, and standards *and* is analyzed using the same set of integrating sphere assumptions as the M_R and M_T measurements, the two sets of measurements are consistent. To put it bluntly, if LabSphere says your sphere has a reflectance of 0.995 and you measure a value of 0.980, I would assert that your value is more appropriate for analyzing your integrating sphere measurements.

5.2.7   Five measurements

```
#lambda  M_R      M_T      M_U     r_w    t_w
 800     0.16830  0.24974  0.0012  0.951  0.980
 810     0.16271  0.00000  0.0000  0.952  0.981 #treated as one measurement
 820     0.16289  0.25530  0.0000  0.953  0.982 #treated as two measurements
```

This is how `iad` handles the case of spheres with different reflectances as a function of wavelength. Typically if the wall re is changing, then so will the sphere wall reflectance. Of course, if the wall reflectance is not changing then just fill in the same value each time. Like the four measurement case, if M_U or M_T is unknown, then just enter zero.

5.2.8   Six measurements

The insanity continues and we allow the reflectance standard to have some spectral character.

```
# nm    M_R    M_T    M_U    r_w    t_w    rstd
 550   0.0731 0.9307 0.0000 0.9788 0.9788 0.9800
```

Typically if the wall reflectance is changing, then so will the standard reflectance. Of course, if the wall reflectance is not changing then just fill in the same value each time. Like the five measurement case, if M_U or M_T is unknown, then just enter zeros.

5.2.9   Seven measurements!

The insanity finally ends. The default transmittance for 100% transmission gets specified also.

```
# nm    M_R    M_T    M_U    r_w    t_w    rstd   tstd
 550   0.0731 0.9307 0.0000 0.9788 0.9788 0.9800 1.0000
```

5.2.10   Putting it all together

```
IAD1
#
# Tests using calculated values for M_R and M_T
# by Scott Prahl
#
1.4            # Index of refraction of sample
1.0            # Index of refraction of top slide
1.0            # [mm] Thickness of sample
1.0            # [mm] Thickness of slides
2.0            # [mm] Diameter of illumination beam
1.00           # Reflectance of calibration standard


0              # [mm] Number of spheres used during each measurement


               # Refection sphere properties (unused because n_spheres=0)
203.2          # [mm] Sphere Diameter
25.4           # [mm] Sample Port Diameter
12.7           # [mm] Entrance Port Diameter
12.7           # [mm] Detector Port Diameter
0.96           # Reflectivity of the sphere wall


               # Transmission sphere properties (unused because n_spheres=0)
203.2          # [mm] Sphere Diameter
25.4           # [mm] Sample Port Diameter
12.7           # [mm] Entrance Port Diameter
12.7           # [mm] Detector Port Diameter
0.96           # Reflectivity of the sphere wall


2              # [mm] Number of measurements


#       M_R             M_T         a    b     g
2.77865808457e-2  1.73065997660e-2 # 0.00 4.0000 0.00
4.20236699283e-2  1.91254597157e-2 # 0.19 4.0000 0.00
6.00960999727e-2  2.19067707658e-2 # 0.36 4.0000 0.00
8.34695920348e-2  2.63617299497e-2 # 0.51 4.0000 0.00
1.14361397922e-1  3.38563099504e-2 # 0.64 4.0000 0.00
1.56228601933e-1  4.70846891403e-2 # 0.75 4.0000 0.00
2.14577898383e-1  7.13708102703e-2 # 0.84 4.0000 0.00
2.97877311707e-1  1.16591498256e-1 # 0.91 4.0000 0.00
4.15349513292e-1  1.96420803666e-1 # 0.96 4.0000 0.00
5.54938077927e-1  3.06980103254e-1 # 0.99 4.0000 0.00
6.29535913467e-1  3.70464086533e-1 # 1.00 4.0000 0.00
```

Table 2: One of the test files `basic4.rxt`. This is a test file with accurately calculated values for M_R and M_T. As a consequence the number of spheres has been set to zero. Other test files in the `test` directory may be helpful starting templates for your data.

6 Running `iad`

The `iad` is run from the command-line. It is typically used with data files that contain values of M_R and M_T as a function of wavelength. `iad` can be used without a data file by using various command-line options or switches (see Table refswitches), but it is reasonably clumsy. In its simplest form one could analyze the data file `basic1.rxt` by typing

```
prompt> iad basic1
```

Note that the extension `.rxt` is automatically appended if necessary. This command will process the data file `basic1.rxt` and produce a file named `basic1.txt`.

6.1   Command-line options

-1 '# # # # #' Five parameters describing the reflection sphere.

> The parameters are the diameters (in mm) of the sphere, the sample port, the entrance port, the detector port, and the reflectivity of the sphere walls. These parameters need to be delimited by single or double quotes and separated by spaces e.g., `-1 '100 10 10 2 0.98'` for a 100 mm sphere with 10 mm diameter sample and entrance ports.

> This option is used for both single and double sphere configurations. If only one sphere is described on the command-line, i.e., there is no `-2` option, then the same parameters are used for the transmission sphere.

-2 '# # # # #' Five parameters describing the transmission sphere.

> The parameters are the diameters (in mm) of the sphere, the sample port, the third port, the detector port, and the reflectivity of the sphere walls. As above, these parameters need to be delimited by single or double quotes and separated by spaces e.g., `-1 '100 10 10 2 0.98'` for a 100 mm sphere with 10 mm diameter sample and third ports.

> The third port is assumed to be on the opposite side of the sphere from the sample port.

> The diameter of third port can be zero which means that the third port is covered with a cap with the same reflectivity as the sphere wall. Usually, a known reflection standard is present in the third port (controlled by the `-T` option described below). If the third port is empty — no unscattered transmitted light is collected by the sphere, then the `-C 0` option should be used so the reflectivity of the third port is zero.

> This option is used for both single and double sphere configurations.

-a # Assume this albedo for all calculations.

> Constrains the inversion process by fixing that the albedo at this value. This is often convenient to use with low scattering `-a 0` and low absorption samples `-a 1` so that a single measurement can be used to determine the absorption coefficient or the scattering coefficient respectively.

> If you want to constrain the reduced albedo $a' = \mu_s(1-g)/[\mu_a + \mu_s(1-g)]$ then use `-g` g together with $a = a'/(1 - g + a' \cdot g)$.

-A # Assume this absorption coefficient for all calculations

> Constrains the inversion process by fixing the absorption coefficient to this value in mm^{-1}. This can be convenient to use with low absorption samples like Intralipid in the visible wavelength range. If two measurements have been made, then `iad` will find the scattering coefficient and the scattering anisotropy. If only a single measurement is available, then just the scattering coefficient will be found assume that $g = 0$ (which can be changed using the `-g` option. so that a single measurement can be

used to determine the absorption coefficient or the scattering coefficient respectively.

-b # Assume this optical thickness for all calculations

Constrains the inversion process by fixing $b = (\mu_a + \mu_s)d$ for the inversion process. This option is useful when doing forward calculations with the `-z` option below.

-B # Assume this beam diameter for all calculations

Constrains the inversion process by fixing the beam diameter to this value in mm. This parameter can be used to determine the effect of the beam diameter on the inversion process. The only way that it enters into the inversion calculation is through the internal Monte Carlo lost light calculation — and so if `-M 0` is used then the option `-b` will have no effect.

-c # The fraction of unscattered reflected light in your reflection `MR` measurement.

This is a number from 0 to 1. Depending on the experiment, the incident beam might be oriented so that all the light reflected at the surface of the sample (or covering slides) is collected `-c 1` or it exits back out the entrance port `-c 0`. If none of the light is collected, then this should be verified by inserting a piece of glass in the sample port and verifying that no light is detected in the sphere. If the light hits the sample at an angle (so that all the light is collected) then the incidence angle option `-i` should also be used.

The default assumes all unscattered reflected light is collected, `-c 1`.

-C # The fraction of unscattered transmitted light in your transmission `MT` measurement.

This is a number from 0 to 1. Depending on the experiment, the third port in the sphere might be closed (or covered by a reflection standard) so that all the unscattered light transmitted through the sample is collected by the sphere `-C 1`. Alternatively, in a double integrating sphere arrangement or when reflected at the surface of the sample (or covering slides) is collected `-c 1` or it exits back out the entrance port `-c 0`. If none of the light is collected, then this should be verified by inserting a piece of glass in the sample port and verifying that no light is detected in the sphere. If the light hits the sample at an angle (so that all the light is collected) then the incidence angle option `-i` should also be used.

The default assumes all unscattered transmitted light is collected, `-C 1`.

-d # The thickness of the sample in mm.

This option is most useful when running the program entirely from the command-line. `iad -r 0.5 -t -0.1 -d 2` will figure out the scattering and absorption for a 2 mm sample with 50% reflection and 10% transmission.

This number enters into the inversion process in two ways. First, during the Monte Carlo lost light calculation that allows light to spread in the sample and possibly escape collection by the integrating sphere. The second is in the very last step in which the absorption and reduced scattering coefficients are calculated from the albedo, optical thickness, and scattering anisotropy, e.g., $\mu_a = (1 - a)b/d$.

The default assumes a 1 mm sample, -d 1.

-D # The thickness of the slides in mm.

This option sets the thickness of the glass slides. This thickness is used only in the Monte Carlo simulations for lost light.

There are two ways of specifying that glass slides were not used in a calculation. The first is to use -D 0 to indicate no thickness. The second is to set the index of refraction of the slides to unity -N 1.

The default assumes no glass slides, -D 0.

-e # The error tolerance for success.

This value determines when the calculated values are close enough. When a single optical property is being determined, like for iad -r 0.5 -g 0, then this is just the difference between the calculated value for MR and the measured value. For two parameters it is more complicated. See §6.3.1 for details.

The default value is 0.0001, -D 0.

-E # The optical absorption depth for the slides.

In the infrared, especially for lime glass, the absorption of the glass slides can be significant. If μ_a^{slides} is the absorption coefficient of the glass slides then the optical absorption depth is the product of this and the thickness of the slide $\mu_a^{slides} \cdot d^{slides}$.

The default value is no slide absorption, -E 0.

-f # The fraction of incident light that hits the sphere wall first

The fraction ranges from 0 to 1. This only applies to reflection measurements. Ideally all the incident light on the sample during the reflection experiment hits the sample first. However, it is possible that due to a small sample size or a large beam or poor collimation, some of the light misses the sample and hits the sphere wall instead.

The default value is that no light hits the wall first, -f 0.

-F # Constrain the scattering coefficient.

The value for this option has three possible cases. First, when the argument is a simple number -F 0.5 then the scattering coefficient is kept fixed at $0.5\,\mathrm{mm}^{-1}$.

The second option is when the value is 'P λ_0 μ_{s0} γ' where the assumed scattering coefficient depends on wavelength according to $\mu_{s0}(\lambda/\lambda_0)^\gamma$. The

value μ_{s0} is the assumed scattering coefficient at λ_0. So the option `-F 'P 1000 1.5 -1.3'` will use the wavelength λ to generate the scattering coefficient $\mu_s = 1.5(\lambda/1000)^{-1.3}$.

The third option is when the value is 'R λ_0 μ_{s0} γ' where the assumed scattering coefficient depends on wavelength according to $\mu_{s0}(\lambda/\lambda_0)^\gamma$. The value μ_{s0} is the assumed scattering coefficient at λ_0. So the option `-F 'R 1000 1.5 -1.3'` will use the wavelength λ to generate the scattering coefficient $\mu'_s = 1.5(\lambda/1000)^{-1.3}$.

-g # Assume this value for the scattering anisotropy for all calculations

Constrains the inversion process by fixing the scattering anisotropy to this value. The program assumes a Henyey-Greenstein scattering phase function and g is the cosine of the average value of the scattering function over all angles. The value ranges from -1 (completely backwards scattering), to 0 (isotropic), to $+1$ (completely forward scattering).

This option is useful when the scattering coefficient is roughly known and only two measurements have been made. For example, using `-g 0.9` for tissue samples is common.

With 1 or 2 measurements the default is isotropic scattering, `-g 0`*.*

-G # type of boundary with various options

-h display help

-H # baffle configuration options

-L # specify the wavelength lambda

-M # number of Monte Carlo iterations

-n # specify index of refraction of slab

-N # specify index of refraction of slides

-o filename explicitly specify filename for output

-p # number of Monte Carlo photons or max MC time in milliseconds

-q # number of quadrature points (default=8)

-r # total reflection measurement

-R # actual reflectance for 100% measurement

-S # number of spheres used

-t # total transmission measurement

-T # actual transmission for 100% measurement

-u # unscattered transmission measurement

-v version information

-V 0 — 1 — 2 verbosity level

-w # wall reflectivity for reflection sphere

-W # wall reflectivity for transmission sphere

-x # set debugging level

-X dual beam configuration

-z do forward calculation

6.2   Basic Program Information

            -h   display help
            -v   version information

These commands are pretty self-explanatory. The `-h` switch lists all the command line options. The `-v` switch just prints the version information of the program.

6.3   Controlling the Analysis

            -e #   error tolerance (default 0.0001)
            -q #   number of quadrature points (default=8)
            -M #   number of Monte Carlo iterations
            -p #   # of Monte Carlo photons (default 100000),
                    (negative number is max time in milliseconds)

6.3.1   The Error Tolerance

The `-e #` option allows you to specify the tolerance for the relative error allowed before the program quits. The default value is 0.0001. It is unlikely that you will need to use this option since the default value seems to work pretty well in general. The relative error used by the program is[23]

$$error = \left| \frac{M_R^{measured} - M_R^{calculated}}{M_R^{measured} + 10^{-6}} \right| + \left| \frac{M_T^{measured} - M_T^{calculated}}{M_T^{measured} + 10^{-6}} \right|$$

As an example, the optical properties for $M_R = 0.3$ and $M_T = 0.1$ for a 1 mm thick sample are found using the command[24]

            prompt> iad -m -r 0.3 -t 0.1

---

[23]The value of 10^{-6} is present to prevent division by zero.

[24]Here I have used the `-m` switch to eliminate the bulk of the output. The eliminated output tells you what sample thickness was assumed and other assumptions made by the program.

which produces

```
      0.3000   0.3000   0.1000   0.1000   0.6730   3.0109   0.0000    0
```

The first two numbers are values for M_R; the first one is measured and exactly matches the second one that is calculated using the given optical properties. The third and fourth numbers are values for M_T and again they match exactly. The next three are the calculated optical properties $\mu_a = 0.67/\text{mm}$, $\mu'_s = 3.01/\text{mm}$, and $g = 0.9$

If the error tolerance is changed to 0.01 then

```
          prompt> iad -m -r 0.3 -t 0.1 -e 0.01
```

produces slightly different optical properties

```
      0.3000   0.3002   0.1000   0.0991   0.6750   3.0229   0.0000    0
```

where the calculated and measured values for M_R nearly match, but the : the measured value of 0.3000 and the calculated value (using the listed optical properties) of 0.3002.

6.3.2   The Number of Monte Carlo Iterations

The `-M #` option allows you to control the *maximum* number of Monte Carlo iterations. The default setting is to do as many Monte Carlo iterations as necessary (up to 20) to ensure that the calculated values for scattering and absorption change by less than $0.01\,\text{mm}^{-1}$ between iterations. Now the number of Monte Carlo iterations is *not* the same as the number of photons used in the Monte Carlo calculation of lost light. Instead, the `-M #` option controls the maximum number of times that the lost light calculation is done.

This option is your friend.[25]   You'll almost always want to turn off the Monte Carlo lost light iterations because the program will run *much, much* faster. Use[26]

```
          prompt> iad -M 0 double
```

until your data file converts and you are reasonably certain that the data is worth spending more time on.

For example if the two sphere data is used `double.rxt` then

```
          prompt> iad double
```

takes 41.9 seconds on my computer. This calculation does at least two Monte Carlo iterations for each of the 21 data points. Now if the Monte Carlo is completely omitted (0 iterations) then

```
          prompt> iad -M 0 double
```

then the calculation only takes 0.3 seconds. Using the option `-M 0` is also handy because it allows you to quickly test the formatting of data files or whether you might have some crazy measurements.

---

[25] `-M 0` is your bonus for reading this far and this deeply in the manual.

[26] `double.rxt` is found in the test directory that shipped with `iad`.

6.3.3   The Number of Monte Carlo Photons

The `-p #` option allows you to specify the number of photons used in the Monte Carlo simulation *or* the length of time that one Monte Carlo iteration should take. The default is 100,000 photons. This option can be handy when you have samples with very low absorption and a single photon takes a long time to propagate. In this case the number of photons can be reduced explicitly. For example, the command

```
prompt> iad -p 10000 double
```

will take only 4.9 seconds. Alternatively, you might find it convenient to limit the calculation time to 100 milliseconds for each Monte Carlo simulation,

```
prompt> iad -p -100 double
```

6.3.4   The Number Quadrature Points

The `-q #` option allows you to specify the number of quadrature points used in the adding-doubling calculation. There are a bunch of integrals that must be calculated numerically; quadrature is an efficient way to do these integrals accurately. `iad` uses a combination of Lobatto and Gaussian quadrature to achieve good results.

The default number of quadrature points or angles is 8. For a variety of reasons, the number of quadrature points should be a multiple of 4. Four quadrature points is more-or-less equivalent to the $\delta - P_3$ approximation. The default value of 8 is accurate for highly anisotropic phase functions and runs quickly.

```
prompt> iad -q 4 double
```

takes only 0.1 seconds. While

```
prompt> iad -q 16 double
```

takes 1.3 seconds.

6.4   Constraining the Optical Properties

Command line constraints allow you to add information to the inversion process.

`-g #`	fixed anisotropy (default 0)
`-a #`	fixed albedo
`-b #`	fixed optical thickness
`-A #`	fixed absorption coefficient
`-F #`	fixed scattering coefficient

6.4.1   Constraining the Scattering Anisotropy

The `-g #` option allows you to control the value of g that is used in the inverse calculation. The default value is 0. This option is particularly useful when you have only made two measurements, but know approximately what the value of the average cosine of the phase function should be. For example,[27]

<div align="center">

```
prompt> iad -r 0.3 -t 0.1
```

</div>

produces

<div align="center">

```
0.3000   0.3000   0.1000   0.1000   0.6730   3.0109   0.0000    0
```

</div>

or $\mu_a = 0.67$/mm, $\mu_s' = 3.01$/mm, and $g = 0.9$. Alternatively, if the value of g is specified then the resulting optical properties are

<div align="center">

```
prompt> iad -r 0.3 -t 0.1 -g 0.9
```

</div>

produces

<div align="center">

```
0.3000   0.3000   0.1000   0.1000   0.5522   3.1601   0.9000    0
```

</div>

or $\mu_a = 0.55$/mm, $\mu_s' = 3.16$/mm, and $g = 0.9$. Interestingly in this example, the reduced scattering coefficient changes by only 5%, but the absorption changes nearly 40%!

6.4.2   Constraining the Albedo

Sometimes it is very handy to specify that the sample is totally absorbing or totally scattering. In this case, one can just type something like

<div align="center">

```
prompt> iad -a 1 -r 0.3
prompt> iad -a 1 -t 0.3
prompt> iad -a 1 -g 0.9 -r 0.3
prompt> iad -a 1 -g 0.9 -t 0.3
prompt> iad -a 0 -t 0.3
```

</div>

6.4.3   Constraining the Optical Thickness

<div align="center">

```
prompt> iad -b 1 -r 0.3
prompt> iad -b 1 -g 0.9 -r 0.3
prompt> iad -b 1 -t 0.5
prompt> iad -b 1 -g 0.9 -t 0.5
```

</div>

Constraining the optical thickness ($b = (\mu_a + \mu_s)d$ where d is the thickness of your sample) is essentially the same as specifying the unscattered transmission through the sample, except that you need not worry about specular reflection at boundaries.

---

[27]Here I have used the `-m` switch to eliminate the bulk of the output. The eliminated output tells you what sample thickness was assumed and other assumptions made by the program.

6.4.4   Constraining the Absorption Coefficient

```
prompt> iad -A 1 -r 0.3
prompt> iad -A 1 -g 0.9 -r 0.3
prompt> iad -A 1 -t 0.3
prompt> iad -A 1 -g 0.9 -t 0.3
prompt> iad -A 1 -r 0.1 -t 0.2
prompt> iad -A 1 -r 0.1 -t 0.2
prompt> iad -A 1 -g 0.9 -r 0.1 -t 0.2
```

Sometimes you know what the absorption coefficient is and it is handy to specify it directly. Oddly the constraint that I use most is the no absorption condition:

```
prompt> iad -A 0 -r 0.3
prompt> iad -A 0 -g 0.9 -r 0.3
prompt> iad -A 0 -t 0.3
prompt> iad -A 0 -g 0.9 -t 0.3
```

This is absurdly handy when dealing with white things like Intralipid and teflon and titanium dioxide samples.

6.4.5   Constraining the Scattering Coefficient

```
prompt> iad -F 1 -r 0.3
prompt> iad -F 1 -g 0.9 -r 0.3
prompt> iad -F 1 -t 0.3
prompt> iad -F 1 -g 0.9 -t 0.3
```

This is probably the least useful of all the constraints, but every once in a while it comes in handy.

6.5   Basic Experimental Description

`-r #`	total reflection measurement
`-t #`	total transmission measurement
`-u #`	unscattered transmission measurement
`-n #`	specify index of refraction of sample
`-N #`	specify index of refraction of slides
`-d #`	physical thickness of the sample
`-D #`	physical thickness of the slides
`-S #`	number of spheres used
`-1 '# # # # #'`	reflection sphere parameters
`-2 '# # # # #'`	transmission sphere parameters

Sometimes it is convenient to analyze data from the command line.

6.5.1   The Measured Reflectance M_R

The `-r #` option allows you to specify a reflectance to be used in the calculation. This number must be between 0 and 1.

6.5.2   The Measured Transmittance M_T

The `-t #` option allows you to specify a transmittance to be used in the calculation. This number must be between 0 and 1.

6.5.3   The Unscattered Transmittance M_U

The `-u #` option allows you to specify a unscattered transmittance to be used in the calculation. This number must be between 0 and 1.

6.5.4   The Index of Refraction of the Slab

The `-n #` option allows you to specify the index of refraction of the sample. This number must be between 0.5 and 2.0. The default is 1.0.

6.5.5   The Index of Refraction of the Glass Slides

The `-N #` option allows you to specify the index of refraction of the glass slides. This number must be between 0.5 and 2.0. The default is 1.0.

6.5.6   The Physical Thickness the Sample

The `-d #` option allows you to specify the physical thickness of the sample. This number must be positive and in millimeters. The default is 1.0 mm.

6.5.7   The Physical Thickness of the Glass Slides

The `-D #` option allows you to specify the thickness of the glass slides. This number should be positive. The default is 0.0 mm which means that there are no glass slides. This thickness is used only in the Monte Carlo simulations to figure out how much light is lost out the edges of the integrating sphere measurements. The units should be millimeters.

6.5.8   The Number of Spheres

The `-S #` option allows you to specify the number of spheres used. This number must be 0, 1, or 2. The default is zero.

6.5.9   The Reflection Sphere Properties

The `-1 '# # # # #'` option allows you to specify the properties of the refection sphere. The five numbers (four diameters and the wall reflectance) must be surrounded by quotes. The five numbers must appear in this order (sphere

diameter, sample port diameter, entrance port diameter, detector port diameter, and sphere wall reflectance). The units should be millimeters.

6.5.10   The Transmission Sphere Properties

The `-1 '# # # # #'` option allows you to specify the properties of the transmission sphere. The five numbers (four diameters and the wall reflectance) must be surrounded by quotes. The five numbers must appear in this order (sphere diameter, sample port diameter, entrance port diameter, detector port diameter, and sphere wall reflectance). The units should be millimeters.

6.6   Controlling the Output

`-o filename`	explicitly specify filename for output
`-V 0`	verbosity low — no output to stderr
`-V 1`	verbosity moderate
`-V 2`	verbosity high
`-x #`	show intermediate calculations

6.6.1   The Output Filename

The `-o filename` option allows you to specify the name of the output file. The default operation is to take the name of the input file and append `.txt` to the name (or if the file ends with `.rxt` then the `.rxt` is replaced by `.txt`). For example,

<div align="center">

`prompt> iad -o foobar double.rxt`

</div>

will put the optical properties for the data in `double.rxt` into the file `foobar`.

6.6.2   Controlling Verbosity

The `-V 0` option allows you to eliminate all the extra output from the `iad` program. This is not used by default. For example,

<div align="center">

`prompt> iad -r 0.3 -t 0.1`

</div>

produces 45 lines of output. The abbreviated output from

<div align="center">

`prompt> iad -V0 -r 0.3 -t 0.1`

</div>

has just one:

```
0.3000   0.3000   0.1000   0.1000   0.6730   3.0109   0.0000    0
```

The `-V 1` option is not so useful when a single line is being processed, but allows one to monitor the process of converting an `.rxt` file into optical properties. These result in the same output[28]

<div align="center">

`prompt> iad vio1`
`prompt> iad -V1 vio1`

</div>

will produce the following on the screen

```
1*1*1*1*1* 1*1*1*1*1* 1*1*1*1*1* 1*1*1*1*1* 1*1*1*1*1*   25 done ( 1.86 s/pt)
1*1*1*1*1* 1*1*1*1*1* 1*1*1*1*1* 1*1*1*1*1* 1*1*1*1*1*   50 done ( 1.64 s/pt)
1*1*1*1*1* 1*1*1*1*1* 1*1*1*1*1* 1*1*1*1*1* 1*1*1*1*1*   75 done ( 1.66 s/pt)
1*1*1*1*1* 1*1*1*1*1* 1*1*1*1*1* 1*1*1*1*1* 1*1*1*1*1*  100 done ( 1.71 s/pt)
1*1*1*1*1* 1*1*1*1*1* 1*1*1*1*1* 1*1*1*1*1* 1*1*1*1*1*  125 done ( 1.74 s/pt)
1*1*1*1*1* 1*1*1*1*1* 1*1*1*1*1* 1*1*1*1*1* 1*1*1*1*1*  150 done ( 1.75 s/pt)
1*1*1*1*1* 1*1*1*1*1* 1*1*1*1*1* 1*1*1*1*1* 1*1*1*1*1*  175 done ( 1.75 s/pt)
1*1*1*1*1* 1*1*1*1*1* 1*1*1*1*1* 1*1*1*1*1* 1*1*1*1*1*  200 done ( 1.75 s/pt)
1*
```

---

[28]`vio1.rxt` is located in the test directory.

(The repeated sequence of `1*` above indicates that one Monte Carlo simulation is done and then the asterisk means that the inversion converged.) The primary reason for doing this is to keep the user informed that processing is taking place. When

<div align="center">

```
prompt> iad -V0 vio1
```

</div>

is used, then nothing is displayed on the screen until the program finishes.

Use `-V 2` is the default. It is just like `-V 1` except it prints a message after processing the file.

6.6.3   Showing Intermediate Calculations

`-x 1`	show sphere and light loss effects
`-x 2`	show grid calculations
`-x 4`	show Monte Carlo iterations
`-x 8`	show lost light
`-x 16`	show sphere effects
`-x 32`	starting guess for optical properties
`-x 64`	show every calculation
`-x 128`	show information about search
`-x 255`	all of the above

6.6.4   Displaying light loss effects

The `-x 1` option allows you to collect an explicit record of how large the light loss effects are for a given calculation. To do this, each data point is analyzed four different ways (1) no sphere corrections and no Monte Carlo light loss corrections, (2) only sphere corrections, (3) only Monte Carlo light loss corrections, and (4) both sets of corrections. It takes a little more than twice as long to analyze the data.

For example the default output for

<div align="center">

```
prompt> iad test/double
```

</div>

reports results like

```
#        Meas    Calc    Meas    Calc    Calc    Calc    Calc    Error
##wave  M_R     M_R     M_T     M_T     mu_a    mu_s'   g       Number
# [nm]  [---]   [---]   [---]   [---]   [1/mm]  [1/mm]  [---]   [---]
 600.0  0.4378  0.4378  0.1808  0.1808  0.0190  0.8708  0.0000  0
 601.0  0.4319  0.4319  0.1754  0.1754  0.0199  0.8702  0.0000  0
 602.0  0.4265  0.4265  0.1706  0.1706  0.0208  0.8681  0.0000  0
...
```

To show the effects of light loss, one uses the command

<div align="center">

```
prompt> iad -x 1 test/double
```

</div>

reports results with the first eight columns as

<div align="center">49</div>

```
#        Meas    Calc    Meas    Calc    Best    Best    Best
##wave   M_R     M_R     M_T     M_T     mu_a    mu_s'   g
# [nm]   [---]   [---]   [---]   [---]   [1/mm]  [1/mm]  [---]
 600.0   0.4378  0.4378  0.1808  0.1808  0.0190  0.8708  0.0000
 601.0   0.4319  0.4319  0.1754  0.1754  0.0199  0.8702  0.0000
 602.0   0.4265  0.4265  0.1706  0.1706  0.0208  0.8679  0.0000
...
```

Where the first column is the wavelength, the next is the measured value for M_R and the third is the value of M_R calculated using the optical properties shown in columns 6–8. The same holds for M_T in columns 4 and 5. The next four columns reveal the amount light lost

```
Lost    Lost    Lost    Lost
R_drct  R_diff  T_drct  T_diff
[---]   [---]   [---]   [1/mm]
0.0051  0.1055  0.0042  0.0364
0.0047  0.1018  0.0040  0.0358
0.0042  0.1020  0.0042  0.0331
...
```

The first column is the light lost directly — collimated light that enters the sample, propagates in the sample and escapes out the front of the sample *but is not collected by the reflectance sphere.* The third column is the amount of this light that exits the back of the sample but is not collected by the transmission sphere. The second column is the amount of lost light arising from light that hits the sample as diffuse light. The two primary sources of this light are light from the source that misses the sample and hits the sphere wall first and light that exits the sample and is collected by the sphere. It is all very annoying.

The remaining columns show the effects that lost light has on the calculated properties of the sample.

```
None    SpOnly  MConly  None    SpOnly  MConly  MC      Error
mu_a    mu_a    mu_a    mu_s'   mu_s'   mu_s'   iter    Number
[1/mm]  [1/mm]  [1/mm]  [1/mm]  [1/mm]  [1/mm]  [---]   [---]
0.0209  0.0201  0.0220  0.6741  0.6739  0.8834  3       0
0.0220  0.0212  0.0228  0.6759  0.6752  0.8829  3       0
0.0230  0.0222  0.0237  0.6773  0.6752  0.8821  3       0
...
```

Slight discrepancies between these results and the previous results are caused by variation in the Monte Carlo simulation. If one looks specifically at the reduced scattering numbers,

```
#        None    SpOnly  MConly  Best
##wave   mu_s'   mu_s'   mu_s'   mu_s'
# [nm]   [1/mm]  [1/mm]  [1/mm]  [1/mm]
 600.0   0.6741  0.6739  0.8834  0.8708
```

```
 601.0  0.6759  0.6752  0.8829  0.8702
 602.0  0.6773  0.6752  0.8821  0.8679
...
```

One sees that the sphere-only corrections decrease the scattering coefficient. That is because the true reflectance is less than the measured value and vice versa for the transmittance. If the true reflectance and transmittance were used then the scattering coefficient would need to decrease which is what happens. Now if light losses are included then both transmittance and reflectance need to increase.

```
#        None    SpOnly  MConly  Best
##wave   mu_a     mu_a   mu_a    mu_a
# [nm]  [1/mm]   [1/mm]  [1/mm]  [1/mm]
 600.0  0.0209  0.0201  0.0220  0.0190
 601.0  0.0220  0.0212  0.0228  0.0199
 602.0  0.0230  0.0222  0.0237  0.0208
...
```

7   Validation

This program has been validated in a number of different ways. The first is using the test files `basic1.rxt`, `basic2.rxt` and `basic3.rxt`. These contain total reflectance and transmittance values for known optical properties.

For example `basic1.rxt` contains

```
#M_R                  #mua  mus  g
0.2992621379268361  #0.1  1.0  0.0
0.1722475379306846  #0.3  1.0  0.0
0.1308339701159747  #0.5  1.0  0.0
0.1096241197070925  #0.7  1.0  0.0
0.0966223181570366  #0.9  1.0  0.0
```

and the output of `iad basic1` is

```
Meas    Calc    Meas    Calc    Calc    Calc    Calc    Error
M_R     M_R     M_T     M_T     mu_a    mu_s'   g       Number
[---]   [---]   [---]   [---]   [1/mm]  [1/mm]  [---]   [---]
0.2993  0.2993  0.0000  0.0000  0.1008  1.0000  0.0000  0
0.1722  0.1722  0.0000  0.0000  0.3022  1.0000  0.0000  0
0.1308  0.1308  0.0000  0.0000  0.5036  1.0000  0.0000  0
0.1096  0.1096  0.0000  0.0000  0.7049  1.0000  0.0000  0
0.0966  0.0966  0.0000  0.0000  0.9062  1.0000  0.0000  0
```

and the absorption coefficients are recovered with an error of about 0.5% when only the reflectance measurement is available.

Tables 4 and 5 show that these results remain valid when experiments with two or three measurements are analyzed. The effect of including spheres is detailed in a paper that will soon be submitted to JBO.

True μ_a [1/mm]	Calc μ_a [1/mm]	True μ'_s [1/mm]	Calc μ'_s [1/mm]
0.1	0.1006	5	4.9840
0.3	0.3016	5	4.9850
0.5	0.5025	5	4.9853
0.7	0.7034	5	4.9853
0.9	0.9042	5	4.9853
0.1	0.1005	10	9.9597
0.3	0.3015	10	9.9613
0.5	0.5024	10	9.9626
0.7	0.7033	10	9.9632
0.9	0.9041	10	9.9642
0.1	0.1005	15	14.9353
0.3	0.3015	15	14.9383
0.5	0.5023	15	14.9417
0.7	0.7033	15	14.9413
0.9	0.9042	15	14.9413
0.1	0.1005	20	19.9106
0.3	0.3015	20	19.9130
0.5	0.5024	20	19.9148
0.7	0.7033	20	19.9169
0.9	0.9041	20	19.9197
0.1	0.1005	25	24.8870
0.3	0.3014	25	24.8929
0.5	0.5024	25	24.8901
0.7	0.7033	25	24.8928
0.9	0.9042	25	24.8947

Table 3: Analysis of `basic2.rxt` that shows an inversion error of approximately 0.5% when two measurements M_R and M_T are available.

True μ_a [1/mm]	Calc μ_a [1/mm]	True μ'_s [1/mm]	Calc μ'_s [1/mm]	True g [—]	Calc g [—]
0.1	0.1008	0.5	0.5035	0.9	0.8993
0.3	0.3023	0.5	0.5017	0.9	0.8996
0.5	0.5045	0.5	0.4995	0.9	0.9000
0.7	0.7072	0.5	0.4969	0.9	0.9005
0.9	0.9105	0.5	0.4940	0.9	0.9010
0.1	0.1007	1.0	0.9994	0.9	0.9000
0.3	0.3023	1.0	0.9976	0.9	0.9002
0.5	0.5041	1.0	0.9955	0.9	0.9004
0.7	0.7061	1.0	0.9932	0.9	0.9006
0.9	0.9085	1.0	0.9909	0.9	0.9008
0.1	0.1007	1.5	1.4967	0.9	0.9002
0.3	0.3022	1.5	1.4949	0.9	0.9003
0.5	0.5037	1.5	1.4929	0.9	0.9004
0.7	0.7055	1.5	1.4909	0.9	0.9006
0.9	0.9073	1.5	1.4888	0.9	0.9007
0.1	0.1007	2.0	1.9938	0.9	0.9003
0.3	0.3020	2.0	1.9921	0.9	0.9004
0.5	0.5035	2.0	1.9903	0.9	0.9005
0.7	0.7050	2.0	1.9885	0.9	0.9006
0.9	0.9066	2.0	1.9865	0.9	0.9006
0.1	0.1007	2.5	2.4910	0.9	0.9004
0.3	0.3020	2.5	2.4896	0.9	0.9004
0.5	0.5033	2.5	2.4880	0.9	0.9005
0.7	0.7047	2.5	2.4862	0.9	0.9005

Table 4: Analysis of `basic3.rxt` that shows an inversion error of approximately 0.5% when three measurements M_R, M_T and M_U are used.

8 Experimental Procedure

1. Prepare your sample. Sandwich it between between glass microscope slides. Use normal saline to improve contact between tissue and glass slides. Do not squish your sample. You may need to use spacers. Refer to section 3.5 for more information about sample preparation.

2. Set up the transmission sphere with the proper port sizes. Generally, you want your sample to be larger than the entrance (sample) port. The beam size to be much smaller than the entrance port size. If you are using an optical fiber to collect light for your detector, then you may need to build or fabricate an insert so that the detector port is completely white except for where the optical fiber is. The diameter of your detector (as used by the program) should be the size of the non-white portion of the collection system.

3. Align your light source and sphere for transmission measurements (right side of Figure 3). Measure your beam size. You will need to make sure that you use the same beam size when making the reflection measurements later.

4. Do the $T(0,0)$ measurement first, followed by T_{dark}. Then place the sample over the entrance port and measure $T(r_s^{direct}, r_s)$. Make sure the baffle is located as shown in Figure 3. Make sure that the sample is flat against the sphere.

5. Change the sphere to make a set of reflectance measurements. You may need to insert your optical fiber in a metal tube (painted white on the outside) so that the fiber face can be placed near your sample. Make sure that your beam diameter is the same as for the transmission experiment.

6. Do the $R(0,0)$ measurement first and try to align so that this measurement is relatively small. Next do the $R(r_{std}, r_{std})$ measurement, make sure that you do not saturate your detector. Finally, place your sample over the sample port and measure $R(r_s^{direct}, r_s)$. Make sure the baffle is located as shown in Figure 3. Make sure that the sample is flat against the sphere.

7. Collect your results into a data file. Prepare the header as outlined in section 5.1. Use equations 2 and 3 to calculate the values for M_R and M_T. Place these values after the header.

8. Convert your data using the `iad` program as outlined in Section 6.

Appendix 1: Error Codes

Error	Description
0	No error
1	The algorithm did not converge after 5000 iterations.
2	Too little reflected light, $M_R < 0$.
3	Too much reflected light, $M_R > 1$.
4	Too little transmitted light, $M_T < 0$.
5	Too much transmitted light, $M_T > 1$.
6	Too little unscattered light, $M_U < 0$.
7	Too much unscattered light, $M_U > 1$.
8	Too much light, $M_R + M_T > 1$.
9	Estimated non-absorbing sample but $M_T > M_U$
10	Estimated unscattered transmittance exceeds M_T
11	Estimated Fresnel reflectance exceeds M_R.
12	Estimated total reflectance $M_R > 1$.
13	Estimated total transmittance $M_T > 1$.
14	Estimated total reflection and transmittance $M_R + M_T > 1$.
15	Estimated total light $M_R + M_T + M_U > 1$.
16	Diameter of sample port is invalid.
17	Diameter of entrance port is invalid.
18	Diameter of detector port is invalid.
19	Reflectance of sphere wall is invalid.
20	Reflectance of detector is invalid.
21	Reflectance of calibration standard is invalid.
22	Internal value γ is not valid.
23	Internal value f (fraction of light hitting the wall first) is invalid.
24	Internal value for phase function is invalid.
25	Value for number of quadrature points must be a multiple of 4.
26	Value for default anisotropy must be $-1 < g < 1$
27	Value for number of layers is too large.
28	Insufficient memory to allocate necessary data structures.
29	File error
30	Too much lost light.
31	Too little reflectance for the measured transmittance

Appendix 2: Optical Properties

Light propagation through tissue is characterized by radiative transport theory with three different optical properties:

- the absorption coefficient μ_a [m^{-1}],

- the scattering coefficient μ_s [m^{-1}], and

- the phase function $p(\hat{s}, \hat{s}')$ [sr^{-1}].

The reciprocal of the absorption or of the scattering coefficient ($1/\mu_a$ or $1/\mu_s$) is the average distance that light will travel before being absorbed or scattered respectively. The phase function describes the fraction of light scattered from the direction $\hat{s}$ into the direction $\hat{s}'$. The phase function is normalized so that its integral over all directions is one,

$$\int_{4\pi} p(\hat{s}, \hat{s}') \, d\omega' = 1.$$

Here $d\omega'$ is a differential solid angle in the $\hat{s}'$ direction. The functional form of the phase function is usually not known. In these cases the phase function is characterized by its average cosine

$$g = \int_{4\pi} p(\hat{s}, \hat{s}')(\hat{s} \cdot \hat{s}') \, d\omega'.$$

The average cosine of the phase function g, is usually called the anisotropy coefficient. The anisotropy coefficient varies between isotropic scattering ($g = 0$) and complete forward scattering ($g = 1$). Notice that the integrals in equations 2 and 3 are independent of the choice of $\hat{s}$. This means that the scattering profile is independent of the incoming light direction. Not surprisingly, a single anisotropy coefficient is inadequate to describe tissues that have special directions along which light scatters better or worse. For example, tissues (e.g., tendon) that have preferential scattering along oriented collagen fibers in a tissue.

The default phase function used by this program is the Henyey-Greenstein

$$p(\cos\theta) = \frac{1}{4\pi} \frac{1 - g^2}{[1 + g^2 - 2g\mu]^{3/2}}$$

Other phase functions can be used, but currently this is the only phase function implemented.

Often the the anisotropy coefficient is not known. In this case the reduced scattering coefficient is useful. It comes from similarity relations that reduce the number of necessary parameters from three down to just two.

$$\mu_s' = (1 - g)\mu_s$$

Appendix 3: Dimensionless Optical Properties

Light propagation is characterized by three parameters: the albedo, the optical depth or thickness, and the phase function. The albedo a is a dimensionless parameter defined as the ratio of scattering coefficient to the sum of scattering and absorption coefficients

$$a = \frac{\mu_s}{\mu_s + \mu_a}$$

The optical depth b is the product of the tissue thickness and the sum of the scattering and absorption coefficients

$$b = \delta(\mu_s + \mu_a).$$

The parameter g is sometimes referred to as the anisotropy coefficient. The scattering coefficient μ_s and the aborption coefficient μ_a are given by

$$\mu_s = \frac{ab}{\delta} \qquad \mu_a = \frac{(1-a)b}{\delta}.$$

The reduced optical albedo and optical depth are given by

$$a' = \frac{a(1-g)}{1 - ag} \qquad b' = (1 - ag)b.$$

The inverse relations are

$$a = \frac{a'}{1 - g + a'g} \qquad b = b' + \frac{a'b'g}{1 - g}.$$

and

$$\mu_s' = \frac{a'b'}{\delta} \qquad \mu_a = \frac{(1-a')b'}{\delta} \qquad \mu_s = \frac{a'b'}{(1-g)\delta}.$$

Appendix 4: Beam and sample size

This appendix is included to show how significant the light loss problem can be. It is excerpted from Niek Van Wieringen's report *The limitations of the determination of optical properties of tissue with a double integrating sphere set-up* (1990). This describes an experiment of some relevance to the issue of selecting a beam size and an integrating sphere port size. It has a few problems, most notably in how the total light measurement was calculated, but the original data is gone so it can't be fixed.

Introduction

One problem associated with making measurements of the optical properties of materials, is light lost out the sides of the sample holder. Lost light leads to erroneously high absorption coefficients because all lost light is attributed to absorption by the sample. The total amount of light collected is the sum of:

- the light specularly reflected out of the reflectance sphere,

- the light collected by the reflectance sphere,

- the light collected by the transmittance sphere, and

- the light transmitted unscattered out of the transmittance sphere.

As light is scattered by the sample some may leave the holder laterally (Figure 6). The amount of light lost will depend on the thickness δ of the sample, the diameter of sphere d, the diameter of the sample port d_s, and the diameter of the beam d_b.

Reflectance and transmittance measurements with a double integrating sphere set-up were used to find the total collected light for non-absorbing samples with
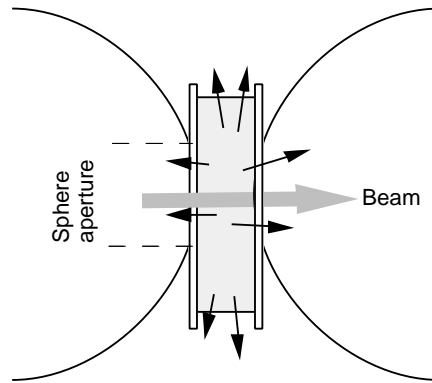

Figure 6: Light losses via the sides of the sample holder. The dashed lines indicate the diameter of the hole in the integrating sphere.

various physical thicknesses δ, scattering coefficients μ_s, and optical thicknesses $\mu_s\delta$. All experiments were done with a 1 mm HeNe laser and various concentrations of Intralipid-10% to create sample optical thicknesses that varied from zero to about 55.

Theory

The straightforward way of figuring out the total light collected would be to add the normalized outputs from the reflectance, diffuse transmittance, and unscattered detectors. The problem is a simple normalization process ignores light losses caused by (1) the absorption by the sphere walls and (2) light exiting out ports is ignored. These effects should be taken into account when using the formulas for a double integrating sphere apparatus. This is what Niek did, but he used the formula for a single integrating sphere to correct his numbers. He also used a slightly incorrect form of this equation and therefore his results will be slightly off (I would guess nor more than 5%). Rather than repeat an incorrect derivation, I'll just skip to the results.

The total light collected was measured for different combinations of the sample port size, different sample thicknesses, and different Intralipid concentrations. The results of these experiments are shown in Figure 7.
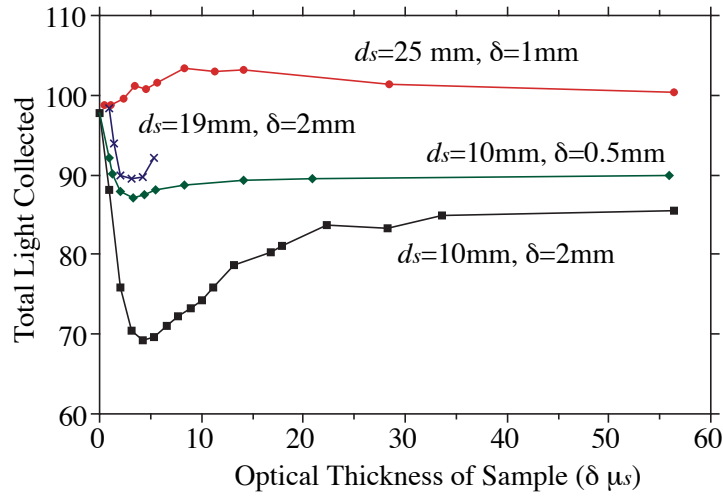

Figure 7: The total collected light versus the optical thickness of the sample. Here δ is the physical thickness of the sample and d_s is the diameter of the sample of the integrating sphere. The beam diameter was 1 mm.

Discussion

The total light collected has roughly the same dependence on the optical thickness for the three smaller port configurations (Figure 7).

1. When the optical thickness is zero, then there is no scattering and no light is lost. (The total amount of light does not equal 100% because the specular reflectance from the sample was not collected.)

2. As the optical thickness increases, more and more light is scattered. More and more light leave out the edges of the sample until a maximum loss is reached.

3. As the optical thickness increases, so does the optical distance in the radial direction. The radial optical thickness eventually increases to the point that the number of scattering events encountered by photons is so large that they travel only a short distance laterally and can no longer escape out the edges.

4. Eventually the radial optical distance becomes so large that no light escapes laterally and the total collected light increases asymptotically to a fixed value.

Consider the curves for a sphere aperture of $d_s = 10\,\mathrm{mm}$. The maximum discrepancy occurs for an optical thickness of about four. When the sample thickness is 2 mm, the total collected light is always less than when the sample thickness is 0.5 mm. The relative radial path lengths are nearly a factor of four greater in the 2 mm case, and photons will encounter four times more scattering events before they might be lost. When the sphere aperture is doubled in size $d_s = 19\,\mathrm{mm}$, then the total light collected is increased for all optical thicknesses.

Summarizing, it appears that:

• the overall collection efficiency is determined primarily by ratio of the radial optical distance to the sample optical thickness,

• the limiting value of for the total light collected as the optical thickness becomes large is primarily determined by the size of the hole in the sphere.

The second point bears closer examination. In short, the argument is because the radial optical distance is always larger than optical depth and therefore as the optical depth becomes large it may be expected that no light can escape via the sides of the sample holder.

However, *light does escape* and one mechanism[29] by which this can happen is via the the glass slides of the holder, as in Figure 8. The circle on the top represents light incident at all angles on a point on the liquid/glass boundary.

---

[29]A second mechanism might be caused by the diffuse light in the integrating sphere. Unlike the relatively small incident beam, all the light in the integrating sphere is diffuse and uniformly impinges on the entire exposed sample surface. The diffuse light that hits near the edge of the port has a roughly 50% chance of being lost. If this lossy rim area is assumed to
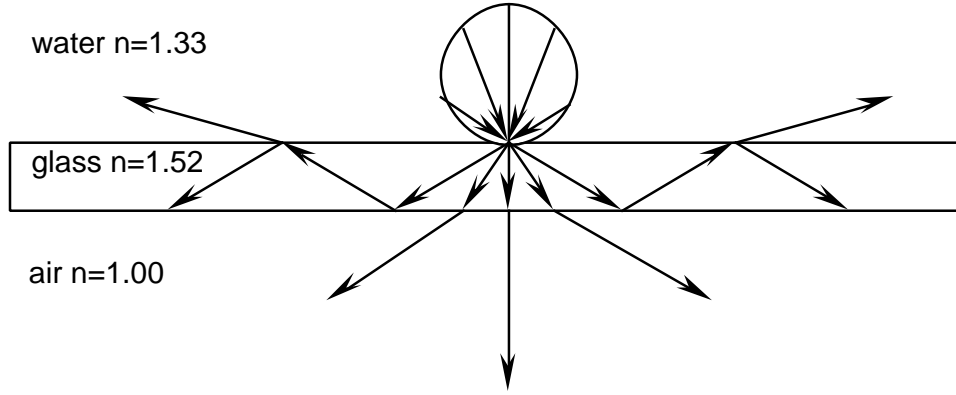
water n=1.33

glass n=1.52

air n=1.00

Figure 8: A glass slide with light incident from all possible angles from the water side. Since there is no critical angle for the water-air transition most light will not be reflected by this boundary. However, total internal reflectance will occur in the glass slide for all light incident at angles greater than 40.5°. This corresponds to angles in the water of greater than 48.8°. Thus any light incident from the water at angles larger than this stand a chance of "walking" down the inside of the glass slide.

The light that passes this boundary makes angles of at most 59.7° with the normal of the slide (represented by the cone inside the glass slide). At the glass-air boundary, light incident at angles larger than the critical angle $\theta_c = 40.49°$ will be reflected totally and otherwise partially. Also at the glass-liquid boundary light will be reflected. If light has been reflected inside the glass slide, a couple of times it will have travelled some distance in the radial direction. For small test apertures the possibility arises that light is conducted sideways and escapes.

This possibility is tested with the following experiment. A thick piece of white perspex, strongly scattering and weakly absorbing, is placed in front of the test aperture of a single sphere set up and percentage of light reflected is measured. This measurement is repeated, this time however with a glass slide against the perspex ('glued' together with a very thin layer of water in order to minimize specular reflectance). The experiment is done for two different sample

be roughly one mean free path wide, then the area is given by

$$\text{lossy rim area} = \frac{\pi d_s}{\mu'_s}$$

The loss will be relative to the total sample area $\pi d_s^2/4$, and consequently we would expect the light losses due to this effect to drop as

$$\frac{\pi d_s/\mu'_s}{\pi d_s^2/4} = \frac{4}{\mu_s d_s} = \frac{1}{\delta \mu_s}\frac{4\delta}{d_s}$$

This means that the losses should continue to decrease with increasing optical thicknesses. This was not observed.

	spot radius	$R = 5\,\mathrm{mm}$	$R = 12.5\,\mathrm{mm}$
without glass	$5 \pm 1\,\mathrm{mm}$	94.3%	94.3%
with glass	$12 \pm 2\,\mathrm{mm}$	83.5%	90.7%

Table 5: The fraction of light collected using a perspex plate with and without a glass slide in front. The spot radius is the size of the glow ball on the perspex. Both experiments used the same beam diameter of $1\,\mathrm{mm}$.

port diameters. The percentage light that is reflected, is shown in table 5.

The values with and without glass slides cannot and should not be directly compared.[30] However, the results for different sample apertures are comparable and more light is lost when a glass slide is present. The glass slide 'conducts' light to the sides of the sample holder.

This is substantiated by another simple experiment that consists of measuring the diameter of the glow ball of scattered light in the perspex plate. When a glass slide is present the glow ball is more than twice the diameter measured with the perspex alone (table 5). A similar effect also appears when Intralipid is used instead of the perspex plate. Thus more light can be recovered by using a larger sample aperture. This effect is present in Figure 6, where the largest sphere aperture gathered the most light. However, for this combination the total percentage of collected light exceeds 100% . This of course is physically impossible, but it has to be taken into account that an approximation is used to determine the percentage of reflected and diffusely transmitted light. Still, this approximation is used in all four combinations and therefore a relation to one remains useful.

---

[30]More light will be transmitted through the sample without glass slides because there are fewer boundaries that can lead to reflected light.

Appendix 5: Beckman UV 5270 Spectrophotometer

Introduction

This memo[31] is intended to describe how reflectance and transmittance experiments might be made with the Beckman UV 5270. Particular attention is paid to the idiosyncrasies and limitations of the Beckman.

First things first. The wavelength is not what it might seem and it should be understood that the number displayed by the Beckman is not the number recorded by the PC attached to the Beckman. For simplicity we [32] choose not to use the digital signal generated by the Beckman, but rather just took the analog signal out of the back and ran it through an A/D board. The output from the A/D board is recorded by the computer.

The measurement need to be divided into four wavelength regions. The UV (250–400 nm), the visible (400–800 nm), the near-infrared (800–1300 nm), and the less-near-infrared (1300–2500 nm). Each will be discussed in turn and skin will be assumed as the sample. However, before we do this some remarks which are applicable regardless of wavelength should be mentioned.

General

- The Beckman should be turned on into the warm-up mode and left there for about 10–15 minutes before turning it on completely. The tungsten lamp is used exclusively except in the UV when the deuterium lamp is needed for extra photo ummph.

- For reflectance measurements, the skin sample is placed against a quartz or glass plate and water was used to match the refractive index of the skin with this plate. Oil was not used[33]. Before performing all measurements a 0% and 99% reflectance scan must be done. Also when doing this scan the 0% and 100% knobs must be adjusted so that the Beckman never reads below 0% or above 100% for either of these scans over the whole wavelength region. Note that the Spectralon reflectance standards should never be put in contact with oil as it renders them defective (they absorb oil, but are hydrophobic). When doing the reference scans no matching fluid or glass/quartz plate is used.

- When performing the transmittance measurements, the sample is placed between two glass or quartz or glass plates. This sample is placed in

---

[31] Vasan Venugopalan at Wellman helped revise this subsection. So he shares the blame and the glory.

[32] Steve Jacques and I spent a week taking data with the Beckman back in 1986. Steve found the A/D converter and I hacked a BASIC program together that week just to get data. This is the pretty much the system that you have now.

[33] Why the worry about oil and water, well if you are interested in hydration effects then it could be an issue. Really, I only considered oil because it has been used on psoriatic lesions to reduce backscattering from the flakey outer layers

front of the sample beam which enters the sphere. In this case a $BaSO_4$ plate is placed in both the sample and reference ports. The 0% and 100% transmittance measurements are performed by placing either an opaque or no sample in the path of the beam. When doing these scans the 0% and 100% knobs must be adjusted so that the Beckman never reads below 0% or above 100% for either of these scans over the whole wavelength region. For the tissue samples, water must also be included to keep the tissue sample hydrated. However when testing epidermis and dermis make sure that the amount of water added does not artificially increase the thickness of the sample. Of course for the transmittance measurements the thickness of the sample must be measured. This is done by measuring the thickness of the quartz/glass plates used with and without the sample inserted in between. You need to make several measurements in different places because most samples are not very uniform in thickness.

- These reference scans should be performed three additional times (e.g., once just before lunch, once after lunch and definitely once just before shutting the machine down for the day.) It is also advisable to scan the 10% or 20% standards at this time if they are to be used for the days measurements. The times when this is necessary will become clearer as you read the rest of this memo.

The Ultraviolet

There are a few problems associated with this region.

- First, the Beckman illuminates with only a single wavelength and detects all light falling on the detector in the integrating sphere. This means that if light is absorbed and the generates fluorescence, much more light will be detected for that wavelength than should be. This was pointed out by Rox, in his (in)famous skin optics paper [119]. Rox used a solar-blind photomultiplier tube (Hamamatsu R456) to prevent detecting visible fluorescence. Thus the same photomultiplier should be used when making the measurements in the wavelength region 250–300 nm. (It should be in one of the drawers in the Beckman room.) Ideally these measurements should also be made with some sort of fluorimeter with the excitation and emission monochromators scanning at the identical speed and wavelength.

- The reflected and transmitted light can be very small (especially for darker skin types). The measurements are correspondingly noisy. We used a 20% reflectance plate as the reference target and adjust the 0% and 100% dials on the Beckman to effectively utilize the full range of the machine. As a result 0–100% will then correspond to a reflectance between 0 and 20%. This improves the generated signal significantly. It might be that the electronics in the Beckman just don't work so well for very small voltages.

- Because glass transmits poorly in this region, quartz plates must be used as the window against which the sample is placed for the reflectance measurement.

- Probably most troubling is that in the ultraviolet region the amount of light falling on the detector is necessarily small. The Beckman opens and closes the slits on the monochromator to ensure that the signal stays reasonably constant. This ensures good signal. Unfortunately, it also increases the bandpass. Watch the dial below the wavelength indicator to get some idea of how large the bandpass is during a typical scan. You might be surprised.

- Of course this is where you need to use the deuterium lamp.

The Visible and Near Infrared (400–1300 nm)

- There is quite a lot of light in this region. The detector begins to fail at around 800 nm (or was it 700 nm?). Anyway the spectrophotometer must be adjusted for infra-red operation. This means that the machine must be turned off, and the setting on the sphere accessory (the lever on the back of the spectrophotometer behind the sphere) switched to IR mono sphere as well as some dinky little switch near the wavelength indicator.

- Once the machine is working in the infrared, you should be aware that the wavelengths now change four times as fast as in the visible. The bandpass indicator is likewise increased in magnitude.

- Also once we are in the infrared you must specify the higher wavelength as the starting wavelength λ_s. The ending wavelength λ_e must be

$$\lambda_e = \lambda_s - \frac{\lambda_s - \lambda_e}{4}$$

because the computer has no idea that the Beckman is operating in the infrared. For example if you want to scan from 800 nm to 2500 nm, You set the dial to 2500 nm and specify the starting wavelength as 2500 nm and the ending wavelength as 2075 nm.

- The scan speed is automatically increased by a factor of 4 once we switch into the IR. Thus scan speed should reduced by depressing the 1/4 nm/s switch from the 4/16 nm/s switch to keep the scan speed at 4 nm/s in the IR.

The Near Infrared (1300–2500 nm)

- The reflectance of skin is very poor in this region. The strong absorption by water in skin is comparable to or exceeds the scattering coefficient. Anyway there is not a whole lot of signal.

66

- The solution once again is to replace the reference plate with a 10 or 20% Spectralon standard. The experiments proceed as for the ultraviolet. The absorption by glass is still pretty small and quartz need not be used.

- The 0% reflectance measurements are a problem. It turns out that the back of the sphere door reflects significant amounts of light in this wavelength range. I remove the door completely and turn off the room lights and sneak off during these calibration scans. All the scans are done in a dark room.

References

[1] S. L. Jacques and S. A. Prahl, "Modeling optical and thermal distributions in tissue during laser irradiation," *Lasers Surg. Med.*, vol. 6, pp. 494–503, 1987.

[2] S. A. Prahl, M. J. C. van Gemert, and A. J. Welch, "Determining the optical properties of turbid media by using the adding-doubling method," *Appl. Opt.*, vol. 32, pp. 559–568, 1993.

[3] T. Moffitt, Y.-C. Chen, and S. A. Prahl, "Preparation and characterization of polyurethane optical phantoms," *Journal of Biomedical Optics*, vol. 11, p. 041103, 2006.

[4] W. F. Cheong, S. A. Prahl, and A. J. Welch, "A review of the optical properties of biological tissues," *IEEE J. Quantum Electron.*, vol. 26, pp. 2166–2185, 1990.

[5] J. W. Pickering, C. J. M. Moes, H. J. C. M. Sterenborg, S. A. Prahl, and M. J. C. van Gemert, "Two integrating sphere with an intervening scattering sample," *J. Opt. Soc. Am. A*, vol. 9, pp. 621–631, 1992.

[6] J. W. Pickering, S. A. Prahl, N. van Wieringen, J. F. Beek, H. J. C. M. Sterenborg, and M. J. C. van Gemert, "Double-integrating-sphere system for measuring the optical-properties of tissue," *Appl. Optics*, vol. 32, pp. 399–410, 1993.

[7] T. Moffitt and S. A. Prahl, "A combined inverse adding-doubling and monte carlo model with experimental correction factors for optical property determination using single and double integrating sphere measurements," *Optics Express*, 2007.

[8] C. Chen, J. Q. Lu, H. F. Ding, K. M. Jacobs, Y. Du, and X. H. Hu, "A primary method for determination of optical parameters of turbid samples and application to intralipid between 550 and 1630 nm," *Opt. Express*, vol. 14, pp. 7420–7435, 2006.

[9] M. Chandra, K. Vishwanath, G. D. Fichter, E. Liao, S. J. Hollister, and M. A. Mycek, "Quantitative molecular sensing in biological tissues: an approach to non-invasive optical characterization," *Opt. Express*, vol. 14, pp. 6157–6171, 2006.

[10] S. C. Gebhart, W. C. Lin, and A. Mahadevan-Jansen, "In vitro determination of normal and neoplastic human brain tissue optical properties using inverse adding-doubling," *Phys. Med. Biol.*, vol. 51, pp. 2011–2027, 2006.

[11] S. C. Mishra, P. Chugh, P. Kumar, and K. Mitra, "Development and comparison of the dtm, the dom and the fvm formulations for the short-pulse laser transport through a participating medium," *Int. J. Heat Mass Transf.*, vol. 49, pp. 1820–1832, 2006.

[12] A. M. De Grand, S. J. Lomnes, D. S. Lee, M. Pietrzykowski, S. Ohnishi, T. G. Morgan, A. Gogbashian, R. G. Laurence, and J. V. Frangioni, "Tissue-like phantoms for near-infrared fluorescence imaging system assessment and the training of surgeons," *J. Biomed. Opt.*, vol. 11, 2006.

[13] K. M. Giraev, N. A. Ashurbekov, and O. V. Kobsev, "Optical spectra of some pathological conditions of stomach tissues," *Int. J. Mod. Phys. B*, vol. 20, pp. 25–36, 2006.

[14] P. R. Bargo, S. A. Prahl, T. T. Goodell, R. A. Sleven, G. Koval, G. Blair, and S. L. Jacques, "In vivo determination of optical properties of normal and tumor tissue with white light reflectance and an empirical light transport model during endoscopy," *J. Biomed. Opt.*, vol. 10, 2005.

[15] A. N. Bashkatov, E. A. Genina, V. I. Kochubey, and V. V. Tuchin, "Optical properties of the subcutaneous adipose tissue in the spectral range 400–2500 nm," *Opt. Spectrosc.*, vol. 99, pp. 836–842, 2005.

[16] M. Itoh, M. Yamanari, Y. Yasuno, and T. Yatagai, "Polarization characteristics of multiple backscattering in human blood cell suspensions," *Opt. Quantum Electron.*, vol. 37, pp. 1277–1285, 2005.

[17] Z. M. Zhao and R. Myllyla, "Measuring the optical parameters of weakly absorbing, highly turbid suspensions by a new technique: photoacoustic detection of scattered light," *Appl. Optics*, vol. 44, pp. 7845–7852, 2005.

[18] D. K. Sardar, R. M. Yow, A. T. C. Tsin, and R. Sardar, "Optical scattering, absorption, and polarization of healthy and neovascularized human retinal tissues," *J. Biomed. Opt.*, vol. 10, 2005.

[19] Y. C. Chen, J. L. Ferracane, and S. A. Prahl, "A pilot study of a simple photon migration model for predicting depth of cure in dental composite," *Dent. Mater.*, vol. 21, pp. 1075–1086, 2005.

[20] S. N. Thennadil and E. B. Martin, "Empirical preprocessing methods and their impact on nir calibrations: a simulation study," *J. Chemometr.*, vol. 19, pp. 77–89, 2005.

[21] M. Jaeger, J. J. Niederhauser, M. Hejazi, and M. Frenz, "Diffraction-free acoustic detection for optoacoustic depth profiling of tissue using an optically transparent polyvinylidene fluoride pressure transducer operated in backward and forward mode," *J. Biomed. Opt.*, vol. 10, 2005.

[22] E. Drakaki, S. Psycharakis, M. Makropolou, and A. A. Serafetinides, "Optical properties and chromophore concentration measurements in tissue-like phantoms," *Opt. Commun.*, vol. 254, pp. 40–51, 2005.

[23] A. N. Bashkatov, E. A. Genina, V. I. Kochubey, and V. V. Tuchin, "Optical properties of human skin, subcutaneous and mucous tissues in the wavelength range from 400–2000 nm," *J. Phys. D-Appl. Phys.*, vol. 38, pp. 2543–2555, 2005.

[24] S. C. Gebhart, A. Mahadevan-Jansen, and W. C. Lin, "Experimental and simulated angular profiles of fluorescence and diffuse reflectance emission from turbid media," *Appl. Optics*, vol. 44, pp. 4884–4901, 2005.

[25] J. C. Ramella-Roman, S. A. Prahl, and S. L. Jacques, "Three monte carlo programs of polarized light transport into scattering media: part i," *Opt. Express*, vol. 13, pp. 4420–4438, 2005.

[26] E. A. Genina, A. N. Bashkatov, V. I. Kochubey, and V. V. Tuchin, "Optical clearing of human dura mater," *Opt. Spectrosc.*, vol. 98, pp. 470–476, 2005.

[27] Y. Liu, Y. L. Kim, and V. Backman, "Development of a bioengineered tissue model and its application in the investigation of the depth selectivity of polarization gating," *Appl. Optics*, vol. 44, pp. 2288–2299, 2005.

[28] T. Collier, M. Follen, A. Malpica, and R. Richards-Kortum, "Sources of scattering in cervical tissue: determination of the scattering coefficient by confocal microscopy," *Appl. Optics*, vol. 44, pp. 2072–2081, 2005.

[29] J. Swartling, J. Svensson, D. Bengtsson, K. Terike, and S. Andersson-Engels, "Fluorescence spectra provide information on the depth of fluorescent lesions in tissue," *Appl. Optics*, vol. 44, pp. 1934–1941, 2005.

[30] B. Choi, L. Tsu, E. Chen, T. S. Ishak, S. M. Iskandar, S. Chess, and J. S. Nelson, "Determination of chemical agent optical clearing potential using *in vitro* human skin," *Lasers Surg. Med.*, vol. 36, pp. 72–75, 2005.

[31] A. Trivedi, S. Basu, and K. Mitra, "Temporal analysis of reflected optical signals for short pulse laser interaction with nonhomogeneous tissue phantoms," *J. Quant. Spectrosc. Radiat. Transf.*, vol. 93, pp. 337–348, 2005.

[32] A. N. Bashkatov, E. A. Genina, V. I. Kochubey, V. V. Tuchin, E. E. Chikina, A. B. Knyazev, and O. V. Mareev, "Optical properties of mucous membrane in the spectral range 350–2000 nm," *Opt. Spectrosc.*, vol. 97, pp. 978–983, 2004.

[33] A. D. Klose, V. Ntziachristos, and A. H. Hielscher, "The inverse source problem based on the radiative transfer equation in optical molecular imaging," *J. Comput. Phys.*, vol. 202, pp. 323–345, 2005.

[34] J. F. Black and J. K. Barton, "Chemical and structural changes in blood undergoing laser photocoagulation," *Photochem. Photobiol.*, vol. 80, pp. 89–97, 2004.

[35] S. M. Maswadi, S. J. Dodd, J. H. Gao, and R. D. Glickman, "Temperature mapping of laser-induced hyperthermia in an ocular phantom using magnetic resonance thermography," *J. Biomed. Opt.*, vol. 9, pp. 711–718, 2004.

[36] D. K. Sardar, F. S. Salinas, J. J. Perez, and A. T. C. Tsin, "Optical characterization of bovine retinal tissues," *J. Biomed. Opt.*, vol. 9, pp. 624–631, 2004.

[37] S. A. Carp, S. A. Prahl, and V. Venugopalan, "Radiative transport in the delta-p-1 approximation: accuracy of fluence rate and optical penetration depth predictions in turbid semi-infinite media," *J. Biomed. Opt.*, vol. 9, pp. 632–647, 2004.

[38] M. H. Khan, B. Choi, S. Chess, K. M. Kelly, J. McCullough, and J. S. Nelson, "Optical clearing of *in vivo* human skin: Implications for light-based diagnostic imaging and therapeutics," *Lasers Surg. Med.*, vol. 34, pp. 83–85, 2004.

[39] B. M. Kim, "Optical property measurements of turbid media using continuous-wave light sources," *J. Korean Phys. Soc.*, vol. 44, pp. 427–434, 2004.

[40] N. Huber, J. Heitz, and D. Bauerle, "Pulsed-laser ablation of polytetrafluoroethylene (ptfe) at various wavelengths," *Eur. Phys. J.-Appl. Phys*, vol. 25, pp. 33–38, 2004.

[41] B. Choi, E. D. Jansen, and A. J. Welch, "Acoustic-based measurements of material absorption coefficients: Relationship between laser pulse duration and stress confinement time," *J. Appl. Phys.*, vol. 94, pp. 7826–7831, 2003.

[42] D. Zhu, Q. M. Luo, and J. A. Cen, "Effects of dehydration on the optical properties of *in vitro* porcine liver," *Lasers Surg. Med.*, vol. 33, pp. 226–231, 2003.

[43] W. C. Lin, C. Buttemere, and A. Mahadevan-Jansen, "Effect of thermal damage on the *in vitro* optical and fluorescence characteristics of liver tissue's," *IEEE J. Sel. Top. Quantum Electron.*, vol. 9, pp. 162–170, 2003.

[44] T. Collier, D. Arifler, A. Malpica, M. Follen, and R. Richards-Kortum, "Determination of epithelial tissue scattering coefficient using confocal microscopy," *IEEE J. Sel. Top. Quantum Electron.*, vol. 9, pp. 307–313, 2003.

[45] C. Das, A. Trivedi, K. Mitra, and T. Vo-Dinh, "Experimental and numerical analysis of short-pulse laser interaction with tissue phantoms containing inhomogeneities," *Appl. Optics*, vol. 42, pp. 5173–5180, 2003.

[46] B. Schulkin, H. C. Lim, N. Guzelsu, G. Jannuzzi, and J. F. Federici, "Polarized light reflection from strained sinusoidal surfaces," *Appl. Optics*, vol. 42, pp. 5198–5208, 2003.

[47] P. Rath, S. C. Mishra, P. Mahanta, U. K. Saha, and K. Mitra, "Discrete transfer method applied to transient radiative transfer problems in participating medium," *Numer. Heat Tranf. A-Appl.*, vol. 44, pp. 183–197, 2003.

[48] J. Swartling, S. Palsson, P. Platonov, S. B. Olsson, and S. Andersson-Engels, "Changes in tissue optical properties due to radio-frequency ablation of myocardium," *Med. Biol. Eng. Comput.*, vol. 41, pp. 403–409, 2003.

[49] F. Fabbri, M. A. Franceschini, and S. Fantini, "Characterization of spatial and temporal variations in the optical properties of tissuelike media with diffuse reflectance imaging," *Appl. Optics*, vol. 42, pp. 3063–3072, 2003.

[50] I. Gannot, A. Garashi, G. Gannot, V. Chernomordik, and A. Gandjbakhche, "In vivo quantitative three-dimensional localization of tumor labeled with exogenous specific fluorescence markers," *Appl. Optics*, vol. 42, pp. 3073–3080, 2003.

[51] T. J. Pfefer, L. S. Matchette, C. L. Bennett, J. A. Gall, J. N. Wilke, A. J. Durkin, and M. N. Ediger, "Reflectance-based determination of optical properties in highly attenuating tissue," *J. Biomed. Opt.*, vol. 8, pp. 206–215, 2003.

[52] G. Zaccanti, F. Martelli, and S. Del Bianco, "Method to measure the optical properties of small volumes of diffusive media," *Appl. Optics*, vol. 41, pp. 7317–7324, 2002.

[53] M. Shimada, J. Hata, Y. Yamada, M. Itoh, A. Uchida, and T. Yatagai, "Experimental and numerical study of the colour appearance of tattoo models," *Med. Biol. Eng. Comput.*, vol. 40, pp. 218–224, 2002.

[54] J. W. Villard, M. D. Feldman, J. Kim, T. E. Milner, and G. L. Freeman, "Use of a blood substitute to determine instantaneous murine right ventricular thickening with optical coherence tomography," *Circulation*, vol. 105, pp. 1843–1849, 2002.

[55] T. P. Moffitt and S. A. Prahl, "Sized-fiber reflectometry for measuring local optical properties," *IEEE J. Sel. Top. Quantum Electron.*, vol. 7, pp. 952–958, 2001.

[56] D. K. Sardar, M. L. Mayo, and R. D. Glickman, "Optical characterization of melanin," *J. Biomed. Opt.*, vol. 6, pp. 404–411, 2001.

[57] A. Sefkow, M. Bree, and M. A. Mycek, "Method for measuring cellular optical absorption and scattering evaluated using dilute cell suspension phantoms," *Appl. Spectrosc.*, vol. 55, pp. 1495–1501, 2001.

[58] M. Shimada, Y. Yamada, M. Itoh, and T. Yatagai, "Melanin and blood concentration in a human skin model studied by multiple regression analysis: assessment by monte carlo simulation," *Phys. Med. Biol.*, vol. 46, pp. 2397–2406, 2001.

[59] Z. X. Guo and S. Kumar, "Discrete-ordinates solution of short-pulsed laser transport in two-dimensional turbid media," *Appl. Optics*, vol. 40, pp. 3156–3163, 2001.

[60] J. K. Barton, G. Frangineas, H. Pummer, and J. F. Black, "Cooperative phenomena in two-pulse, two-color laser photocoagulation of cutaneous blood vessels," *Photochem. Photobiol.*, vol. 73, pp. 642–650, 2001.

[61] D. K. Sardar, R. M. Yow, and M. L. Mayo, "Optical characterization of a laser dye in a solid state host," *J. Appl. Phys.*, vol. 89, pp. 7739–7744, 2001.

[62] T. L. Troy and S. N. Thennadil, "Optical properties of human skin in the near infrared wavelength range of 1000–2200 nm," *J. Biomed. Opt.*, vol. 6, pp. 167–176, 2001.

[63] R. K. Shah, B. Nemati, L. H. V. Wang, and S. M. Shapshay, "Optical-thermal simulation of tonsillar tissue irradiation," *Lasers Surg. Med.*, vol. 28, pp. 313–319, 2001.

[64] Y. Du, X. H. Hu, M. Cariveau, X. Ma, G. W. Kalmus, and J. Q. Lu, "Optical properties of porcine skin dermis between 900 nm and 1500 nm," *Phys. Med. Biol.*, vol. 46, pp. 167–181, 2001.

[65] M. Shimada, Y. Masuda, Y. Yamada, M. Itoh, M. Takahashi, and T. Yatagai, "Explanation of human skin color by multiple linear regression analysis based on the modified lambert-beer law," *Opt. Rev.*, vol. 7, pp. 348–352, 2000.

[66] J. I. Youn, S. A. Telenkov, E. Kim, N. C. Bhavaraju, B. J. F. Wong, J. W. Valvano, and T. E. Milner, "Optical and thermal properties of nasal septal cartilage," *Lasers Surg. Med.*, vol. 27, pp. 119–128, 2000.

[67] M. Morin, S. Verreault, A. Mailloux, J. Frechette, S. Chatigny, Y. Painchaud, and P. Beaudry, "Inclusion characterization in a scattering slab with time-resolved transmittance measurements: perturbation analysis," *Appl. Optics*, vol. 39, pp. 2840–2852, 2000.

[68] J. S. Dam, T. Dalgaard, P. E. Fabricius, and S. Andersson-Engels, "Multiple polynomial regression method for determination of biomedical optical properties from integrating sphere measurements," *Appl. Optics*, vol. 39, pp. 1202–1209, 2000.

[69] J. K. Barton, G. Vargas, T. J. Pfefer, and A. J. Welch, "Laser fluence for permanent damage of cutaneous blood vessels," *Photochem. Photobiol.*, vol. 70, pp. 916–920, 1999.

[70] G. Balgi, J. Reynolds, R. H. Mayer, R. E. Cooley, and E. M. Sevick-Muraca, "Measurements of multiply scattered light for on-line monitoring of changes in size distribution of cell debris suspension," *Biotechnol. Prog.*, vol. 15, pp. 1106–1114, 1999.

[71] G. de Vries, J. F. Beek, G. W. Lucassen, and M. J. C. van Gemert, "The effect of light losses in double integrating spheres on optical properties estimation," *IEEE J. Sel. Top. Quantum Electron.*, vol. 5, pp. 944–947, 1999.

[72] J. K. Barton, D. X. Hammer, T. J. Pfefer, D. J. Lund, B. E. Stuck, and A. J. Welch, "Simultaneous irradiation and imaging of blood vessels during pulsed laser delivery," *Lasers Surg. Med.*, vol. 24, pp. 236–243, 1999.

[73] W. H. Nau, R. J. Roselli, and D. F. Milam, "Measurement of thermal effects on the optical properties of prostate tissue at wavelengths of 1,064 and 633 nm," *Lasers Surg. Med.*, vol. 24, pp. 38–47, 1999.

[74] A. R. Jones, "Light scattering for particle characterization," *Prog. Energy Combust. Sci.*, vol. 25, pp. 1–53, 1999.

[75] C. R. Simpson, M. Kohl, M. Essenpreis, and M. Cope, "Near-infrared optical properties of *ex vivo* human skin and subcutaneous tissues measured using the monte carlo inversion technique," *Phys. Med. Biol.*, vol. 43, pp. 2465–2478, 1998.

[76] K. Michielsen, H. De Raedt, J. Przeslawski, and N. Garcia, "Computer simulation of time-resolved optical imaging of objects hidden in turbid media," *Phys. Rep.-Rev. Sec. Phys. Lett.*, vol. 304, pp. 90–144, 1998.

[77] D. K. Sardar and L. B. Levy, "Optical properties of whole blood," *Lasers Med. Sci.*, vol. 13, pp. 106–111, 1998.

[78] C. L. Smithpeter, A. K. Dunn, A. J. Welch, and R. Richards-Kortum, "Penetration depth limits of *in vivo* confocal reflectance imaging," *Appl. Optics*, vol. 37, pp. 2749–2754, 1998.

[79] W. Verkruysse, A. M. K. Nilsson, T. E. Milner, J. F. Beek, G. W. Lucassen, and M. J. C. van Gemert, "Optical absorption of blood depends on temperature during a 0.5 ms laser pulse at 586 nm," *Photochem. Photobiol.*, vol. 67, pp. 276–281, 1998.

[80] S. L. Jacques, "Light distributions from point, line and plane sources for photochemical reactions and fluorescence in turbid biological tissues," *Photochem. Photobiol.*, vol. 67, pp. 23–32, 1998.

[81] N. Fukshansky-Kazarinova, L. Fukshansky, M. Kuhl, and B. B. Jorgensen, "Solution of the inverse problem of radiative transfer on the basis of measured internal fluxes," *J. Quant. Spectrosc. Radiat. Transf.*, vol. 59, pp. 77–89, 1998.

[82] J. F. Beek, P. Blokland, P. Posthumus, M. Aalders, J. W. Pickering, H. J. C. M. Sterenborg, and M. J. C. van Gemert, "In vitro double-integrating-sphere optical properties of tissues between 630 and 1064 nm," *Phys. Med. Biol.*, vol. 42, pp. 2255–2261, 1997.

[83] V. V. Tuchin, "Light scattering study of tissues," *Uspekhi Fiz. Nauk*, vol. 167, pp. 517–539, 1997.

[84] E. K. Chan, B. Sorg, D. Protsenko, M. Oneil, M. Motamedi, and A. J. Welch, "Effects of compression on soft tissue optical properties," *IEEE J. Sel. Top. Quantum Electron.*, vol. 2, pp. 943–950, 1996.

[85] H. J. van Staveren, R. H. P. Bertrams, and W. M. Star, "Bladder pdt with intravesical clear and light scattering media: Effect of an eccentric isotropic light source on the light distribution," *Lasers Surg. Med.*, vol. 20, pp. 248–253, 1997.

[86] J. M. C. C. Coremans, C. Ince, H. A. Bruining, and G. J. Puppels, "(semi-)quantitative analysis of reduced nicotinamide adenine dinucleotide fluorescence images of blood-perfused rat heart," *Biophys. J.*, vol. 72, pp. 1849–1860, 1997.

[87] A. M. K. Nilsson, G. W. Lucassen, W. Verkruysse, S. AnderssonEngels, and M. J. C. van Gemert, "Changes in optical properties of human whole blood *in vitro* due to slow heating," *Photochem. Photobiol.*, vol. 65, pp. 366–373, 1997.

[88] I. V. Yaroslavsky, A. N. Yaroslavsky, T. Goldbach, and H. J. Schwarzmaier, "Inverse hybrid technique for determining the optical properties of turbid media from integrating-sphere measurements," *Appl. Optics*, vol. 35, pp. 6797–6809, 1996.

[89] R. RichardsKortum and E. SevickMuraca, "Quantitative optical spectroscopy for tissue diagnosis," *Annu. Rev. Phys. Chem.*, vol. 47, pp. 555–606, 1996.

[90] A. Sadhwani, K. T. Schomacker, G. J. Tearney, and N. S. Nishioka, "Determination of teflon thickness with laser speckle.1. potential for burn depth diagnosis," *Appl. Optics*, vol. 35, pp. 5727–5735, 1996.

[91] E. Chan, T. Menovsky, and A. J. Welch, "Effects of cryogenic grinding on soft-tissue optical properties," *Appl. Optics*, vol. 35, pp. 4526–4532, 1996.

[92] B. Nemati, H. G. Rylander, and A. J. Welch, "Optical properties of conjunctiva, sclera, and the ciliary body and their consequences for transscleral cyclophotocoagulation," *Appl. Optics*, vol. 35, pp. 3321–3327, 1996.

[93] W. C. Lin, M. Motamedi, and A. J. Welch, "Dynamics of tissue optics during laser heating of turbid media," *Appl. Optics*, vol. 35, pp. 3413–3420, 1996.

[94] H. J. van Staveren, H. P. A. Marijnissen, M. C. G. Aalders, and W. M. Star, "Construction, quality assurance and calibration of spherical isotropic fibre optic light diffusers," *Lasers Med. Sci.*, vol. 10, pp. 137–147, 1995.

[95] H. J. van Staveren, M. Keijzer, T. Keesmaat, H. Jansen, W. J. Kirkel, J. F. Beek, and W. M. Star, "Integrating sphere effect in whole-bladder-wall photodynamic therapy.3. fluence multiplication, optical penetration and light distribution with an eccentric source for human bladder optical properties," *Phys. Med. Biol.*, vol. 41, pp. 579–590, 1996.

[96] C. M. Gardner, S. L. Jacques, and A. J. Welch, "Fluorescence spectroscopy of tissue: Recovery of intrinsic fluorescence from measured fluorescence," *Appl. Optics*, vol. 35, pp. 1780–1792, 1996.

[97] I. S. Saidi, S. L. Jacques, and F. K. Tittel, "Mie and rayleigh modeling of visible-light scattering in neonatal skin," *Appl. Optics*, vol. 34, pp. 7410–7418, 1995.

[98] S. G. Proskurin, Y. Yamada, and Y. Takahashi, "Absorption-coefficient measurements of strongly scattering media using time-resolved transmittance of a short-pulse in near-infrared (nir) wavelength range," *Opt. Rev.*, vol. 2, pp. 292–297, 1995.

[99] D. G. Papaioannou, G. W. Thooft, J. J. M. Baselmans, and M. J. C. van Gemert, "Image quality in time-resolved transillumination of highly scattering media," *Appl. Optics*, vol. 34, pp. 6144–6157, 1995.

[100] H. J. van Staveren, J. F. Beek, M. Keijzer, and W. M. Star, "Integrating sphere effect in whole-bladder-wall photodynamic therapy.2. the influence of urine at 458, 488, 514 and 630 nm optical irradiation," *Phys. Med. Biol.*, vol. 40, pp. 1307–1315, 1995.

[101] A. M. K. Nilsson, R. Berg, and S. Anderssonengels, "Measurements of the optical-properties of tissue in conjunction with photodynamic therapy," *Appl. Optics*, vol. 34, pp. 4609–4619, 1995.

[102] P. Marquet, F. Bevilacqua, C. Depeursinge, and E. B. Dehaller, "Determination of reduced scattering and absorption-coefficients by a single charge-coupled-device array measurement.1. comparison between experiments and simulations," *Opt. Eng.*, vol. 34, pp. 2055–2063, 1995.

[103] M. H. Eddowes, T. N. Mills, and D. T. Delpy, "Monte-carlo simulations of coherent backscatter for identification of the optical coefficients of biological tissues in-vivo," *Appl. Optics*, vol. 34, pp. 2261–2267, 1995.

[104] C. J. Hourdakis and A. Perris, "A monte-carlo estimation of tissue optical-properties for use in laser dosimetry," *Phys. Med. Biol.*, vol. 40, pp. 351–364, 1995.

[105] J. N. Qu, C. Macaulay, S. Lam, and B. Palcic, "Optical-properties of normal and carcinomatous bronchial tissue," *Appl. Optics*, vol. 33, pp. 7397–7405, 1994.

[106] J. W. Pickering, P. Posthumus, and M. J. C. van Gemert, "Continuous measurement of the heat-induced changes in the optical-properties (at 1,064-nm) of rat-liver," *Lasers Surg. Med.*, vol. 15, pp. 200–205, 1994.

[107] V. V. Tuchin, S. R. Utz, and I. V. Yaroslavsky, "Tissue optics, light-distribution, and spectroscopy," *Opt. Eng.*, vol. 33, pp. 3178–3188, 1994.

[108] H. J. van Staveren, J. F. Beek, J. W. H. Ramaekers, M. Keijzer, and W. M. Star, "Integrating sphere effect in whole bladder wall photodynamic therapy. 1. 532 nm versus 630 nm optical irradiation," *Phys. Med. Biol.*, vol. 39, pp. 947–959, 1994.

[109] A. J. Durkin, S. Jaikumar, and R. Richardskortum, "Optically dilute, absorbing, and turbid phantoms for fluorescence spectroscopy of homogeneous and inhomogeneous samples," *Appl. Spectrosc.*, vol. 47, pp. 2114–2121, 1993.

[110] J. W. Pickering, S. Bosman, P. Posthumus, P. Blokland, J. F. Beek, and M. J. C. van Gemert, "Changes in the optical-properties (at 632.8 nm) of slowly heated myocardium," *Appl. Optics*, vol. 32, pp. 367–371, 1993.

[111] D. D. Royston, R. S. Poston, and S. A. Prahl, "Optical properties of scattering and absorbing materials used in the development of optical phantoms at 1064 nm," *J. Biomedical Optics*, vol. 1, pp. 110–116, 1996.

[112] W. E. Sumpner, "The diffusion of light," *Proc. Phys. Soc. London*, vol. 12, pp. 10–29, 1892.

[113] R. Ulbricht, "Die bestimmung der mittleren räumlichen lichtintensität durch nur eine messung," *Elektrotechnische Zeitschrift*, vol. 21, pp. 595–597, 1900.

[114] A. H. Taylor, "Measurement of diffuse reflection factors and a new absolute reflectometer," *Sci. Papers Bur. Std.*, vol. S16, pp. 421–436, 1920.

[115] J. A. Jacquez and H. F. Kuppenheim, "Theory of the integrating sphere," *J. Opt. Soc. Am.*, vol. 45, pp. 460–470, 1955.

[116] D. G. Goebel, "Generalized integrating sphere theory," *Appl. Opt.*, vol. 6, pp. 125–128, 1967.

[117] W. W. Wendland and H. G. Hecht, *Reflectance Spectroscopy*. New York: Interscience Publishers, 1966.

[118] S. L. Jacques, C. A. Alter, and S. A. Prahl, "Angular dependence of Hene laser light scattering by human dermis," *Lasers Life Sci.*, vol. 1, pp. 309–333, 1987.

[119] R. R. Anderson and J. A. Parrish, "The optics of human skin," *J. Invest. Dermatol.*, vol. 77, pp. 13–19, 1981.